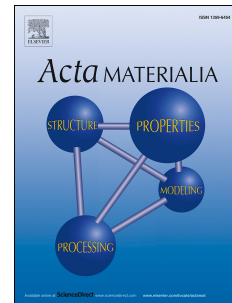


Accepted Manuscript

Enumeration of the Hydrogen-Enhanced Localized Plasticity Mechanism for Hydrogen Embrittlement in Structural Materials

May L. Martin, Mohsen Dadfarnia, Akihide Nagao, Shuai Wang, Petros Sofronis



PII: S1359-6454(18)30956-X

DOI: <https://doi.org/10.1016/j.actamat.2018.12.014>

Reference: AM 15022

To appear in: *Acta Materialia*

Received Date: 10 September 2018

Revised Date: 6 December 2018

Accepted Date: 9 December 2018

Please cite this article as: M.L. Martin, M. Dadfarnia, A. Nagao, S. Wang, P. Sofronis, Enumeration of the Hydrogen-Enhanced Localized Plasticity Mechanism for Hydrogen Embrittlement in Structural Materials, *Acta Materialia*, <https://doi.org/10.1016/j.actamat.2018.12.014>.

This is a PDF file of an unedited manuscript that has been accepted for publication. As a service to our customers we are providing this early version of the manuscript. The manuscript will undergo copyediting, typesetting, and review of the resulting proof before it is published in its final form. Please note that during the production process errors may be discovered which could affect the content, and all legal disclaimers that apply to the journal pertain.

Enumeration of the Hydrogen-Enhanced Localized Plasticity Mechanism for Hydrogen Embrittlement in Structural Materials

May L. Martin^{1,2,3}, Mohsen Dadfarnia^{1,4,5}, Akihide Nagao^{1,4,6}, Shuai Wang^{1,7,8}, Petros Sofronis^{1,4,*}

¹ International Institute for Carbon-Neutral Energy Research (WPI-I2CNER), Kyushu University, 744 Motooka, Nishi-ku, Fukuoka, Fukuoka 819-0395, Japan

² Applied Chemicals and Materials Division, Material Measurement Laboratory, National Institute of Standards and Technology (NIST), 325 Broadway, Boulder, CO 80305, USA

³ Department of Physics, University of Colorado, Boulder, Colorado 80309, USA

⁴ Department of Mechanical Science and Engineering, University of Illinois at Urbana-Champaign, 1206 West Green Street, Urbana, IL 61801, USA

⁵ Department of Mechanical Engineering
Seattle University
901 12th Ave, Seattle, WA 98122-1090

⁶ Material Surface & Interface Science Research Department, Steel Research Laboratory, JFE Steel Corporation, Minamiwatarida-cho, Kawasaki-ku, Kawasaki, Kanagawa 210-0855, Japan

⁷ Department of Engineering Physics, University of Wisconsin-Madison, 1415 Engineering Drive, Madison, WI 53706, USA

⁸ Department of Mechanical and Energy Engineering, Southern University of Science and Technology, 1088 Xueyuan Blvd, Shenzhen 518055, China

* Corresponding author, Tel. +1-217-333-2636, fax +1-217-244-6534, Email address: sofronis@illinois.edu.

Abstract

This paper presents a review of recent experimental evidence and simulation results enumerating the development of the hydrogen-enhanced localized plasticity (HELP) mechanism as a viable hydrogen embrittlement mechanism for structural materials. A wide range of structural materials, including ferritic, martensitic, and austenitic steels, iron, and nickel are covered by the studies reviewed here, as are a variety of mechanical loading conditions and hydrogen charging conditions, supporting the concept that, despite differences in failure mode, there is a universality to the HELP mechanism.

Keywords: Hydrogen embrittlement; HELP; Steel; Failure; Continuum and atomistic simulations

1. Introduction

The premature failure of metallic components due to hydrogen embrittlement continues to plague industry, despite our knowing for over a century that hydrogen is the cause. Hydrogen embrittlement continues to be a controversial scientific topic that is subject to a considerable number of studies, as the primary mechanism by which it operates is still under debate. The vitality of this field was evident at the recent International Hydrogen Conference in Jackson Hole, USA (September 11-14, 2016) [1]. The conference revealed a great deal of new data and interpretations, but also highlighted what still remains to be done to consolidate the field to a common understanding of the mechanism(s), and the best way to apply it to material selection and design for hydrogen compatibility.

Since the discovery of hydrogen embrittlement in 1874 [2], many mechanisms have been proposed and discarded as new evidence has been uncovered (see e.g. [3,4] for an overview). One of the primary disputes between different camps is the role of plasticity in hydrogen embrittlement. As the name suggests, hydrogen embrittlement results in a loss in ductility, and often includes a transition to a brittle fracture mode, such as intergranular failure. On such macroscopic scales, the phenomenon seems aptly named as embrittlement. However, more recently, new evidence suggests that there is a notable amount of plasticity associated with these

failures, though not always evident outside of the microscale. The current argument rests on the importance of this plasticity: whether it is crucial to the embrittlement process or simply a minimal and secondary result of the hydrogen-induced failure. This review focuses on a mechanism predicated on plasticity being crucial to the embrittlement process: Hydrogen Enhanced Localized Plasticity (HELP), with emphasis on recent results which address how this enhanced local plasticity may lead to macroscopically brittle behavior.

2. HELP mechanism

The concept of hydrogen enhanced plasticity was first proposed by Beachem in 1972 [5], and has been expanded by the work of Birnbaum and coworkers [6–10]. The premise of the mechanism is that hydrogen assists the deformation processes, but only locally where hydrogen is present in sufficient concentrations, leading to fracture which is macroscopically brittle in appearance and behavior.

Hydrogen is strongly bound to dislocation cores, most likely due to vacancy-like defects at the core [11,12], as well as the attraction to the elastic field surrounding the dislocation. This results in the formation of an atmosphere of hydrogen, which can resemble Cottrell carbon atmospheres [13–16]. In a very specific material-dependent temperature and strain-rate range [13,14,17], the hydrogen atmospheres have a unique effect on the dislocation behavior: dislocation motion is found to be accelerated in the presence of hydrogen. Hydrogen-enhanced dislocation motion has been observed directly through *in-situ* transmission electron microscopy (TEM) observations [7,18–20], and indirectly through stress relaxation tests [21,22] and uniaxial tensile tests [23–26]. The temperature and strain-rate range for this acceleration of dislocation motion tends to correspond to the range of conditions at which the materials are susceptible to hydrogen embrittlement [13]. Outside of this temperature and strain-rate range, pinning and serrated yielding behavior due to the presence of hydrogen have been reported [27–29], as expected due to solute drag behavior similar to the effect of other interstitial solutes, such as carbon.

It is important to note that the presence of hydrogen around the dislocations will result in several important changes in dislocation behavior. The mobility of the dislocations is usually increased, with 2-10 fold increases having been recorded, depending upon the material [17,30],

and with the effect being more pronounced in solute strengthened materials. Additionally, the dislocations will tend to pack closer together [9], particularly in pile-ups. Furthermore, as the atmospheres primarily form due to the tension field of edge dislocations, they stabilize the edge components, thereby reducing the tendency for cross-slip [19,31]; an effect possibly compounded by a reduction in stacking fault energy due to the presence of hydrogen [19,32].

Two reasons are proposed for this increased dislocation mobility. The first applies more to edge dislocations: the hydrogen atmosphere surrounding the dislocation core alters the stress field of the dislocation, affecting its motion by creating a shielding effect and changing the interaction energy between dislocations and obstacles [7,13,20,31], such as secondary phases, solute atoms, and other dislocations. It is this reduction in interaction energy which increases the mobility, by allowing dislocation motion at lower stresses. The second, advanced by Kirchheim and co-workers, is based upon thermodynamic considerations which would apply to all dislocations: hydrogen segregated to dislocations lowers their formation energy [33–36]. One consequence of this reduction in formation energy will be an enhancement in the nucleation rates of dislocation kink-pairs [23,37–42]. If kink-pair formation is considered as the rate-limiting step for dislocation motion, higher nucleation rates would result in increased dislocation mobility [34].

The question has been how this hydrogen-influenced dislocation behavior leads to accelerated brittle-like failure, and, until recently, this question has remained unanswered. This review summarizes recent experimental evidence, focusing on results from new fractographic analysis techniques, as well as related simulations, and discusses the viability of the HELP mechanism as an explanation for hydrogen-enhanced failure in structural materials.

3. HELP and microstructure

As described above, solute hydrogen impacts the mobility of dislocations in most metals, but, unlike other interstitial atoms which create solute drag, hydrogen can cause an increase in dislocation mobility [13,14,19,22,43]. The expected result would be a difference in the developing microstructure during mechanical loading. The increased mobility of dislocations with hydrogen would be predicted to result in higher dislocation densities than in its absence at equivalent strains, which would also be more easily accommodated by the closer packing

encouraged by the presence of hydrogen. Indeed, this is the case observed in cold-rolled palladium [33,44], where multiple techniques confirmed the higher dislocation density at the same strain in samples cold-rolled in the presence of hydrogen compared to samples cold-rolled in its absence. Examination of the microstructure revealed tighter packing of the dislocations in the presence of hydrogen. Under the conditions in which clear cell structures were observed both in the absence and presence of hydrogen, the cell walls in the Pd-H samples were clearly thicker and tighter packed, resulting in a greater degree of crystal rotation between the cells, and the cells themselves appeared smaller in size [44]. Similar results were found in nickel samples subjected to high-pressure torsion processing, both in the presence and absence of hydrogen [45]. Increased dislocation activity was also observed in vanadium micropillars compressed in the presence of hydrogen [46].

As hydrogen also impacts other aspects of the behavior of dislocations than simply mobility, such as reducing the tendency for cross-slip [19,20,31], it would also be expected that there could be differences in the microstructural evolution with strain. Delafosse [47] observed that, in single crystal nickel after 0.75 plastic shear strain, the microstructure was indicative of the stage III regime (equiaxed dislocation cell structures), while it was still only indicative of stage II (planar structures) in the presence of hydrogen. This difference in microstructural evolution was also reflected in the differences in the stress-strain behavior. It is possible that the influence of hydrogen on the dislocation behavior can also result in the stabilization of certain dislocation geometries, resulting in a delay in the transition between different stages of dislocation structure evolution [48], but this requires further study.

The first suggestion of a plasticity based mechanism for hydrogen embrittlement was based on the examination of fracture surfaces [5], and was firmly established through dislocation-based studies [19,20]. However, the difficulty has always been in linking these two length scales, and explaining how increased dislocation activity can result in brittle-appearing fracture features. Focused ion beam (FIB) fabrication of site-specific transmission electron microscopy (TEM) samples allows correlation of dislocation/microstructural features and fracture surface topology, from which inferences into the fracture processes can be made. In the following sections, several case studies of hydrogen embrittlement failures by different modes in different materials are discussed, and it will be shown that a common thread unites them, with strong support for HELP being active.

3.1. “Quasi-cleavage” failure in iron and ferritic steels

Iron and ferritic steels tend to transition from a ductile microvoid coalescence fracture mode to a “brittle”-appearing transgranular “quasi-cleavage” mode in the presence of hydrogen. This has often been associated with a similar phenomenon of the ductile-to-brittle transition that occurs at low temperature [49]. The very application of the term “quasi-cleavage” suggests a cleavage-like process, but not occurring along a cleavage plane. For example, an initial examination of the fracture surfaces in a ferritic high strength low alloy steel (Fig. 1) suggests features that are macroscopically flat. However, high magnification scanning electron microscopy (SEM) of the features shows that they are not flat. The surface is curved, almost undulating, such that no fracture plane can be assigned. On top of this curvature, very fine (100 nm) features exist, suggestive of either mounds or dimples on the surface (Fig. 1b). Underneath this surface, an extremely high density of dislocations exists (Fig. 1c). This evenly dense set of dislocations is complicated, with a spacing on the same order as the size of the fine features on the fracture surface, and extends for at least 10 micrometers (extent of the TEM sample), from the fracture surface and through grain boundaries without variation, suggesting it extends even deeper [50]. The extent of the plasticity negates the idea that either this plasticity is purely surface related, or that it is due to a particularly small constrained plastic zone. It suggests that many slip systems were active over an extensive area, with hydrogen enhancing the dislocation motion. With continuing dislocation motion, hydrogen accumulated in the grain, until the weakest path through the grain failed. The evidence suggests that the term “quasi-cleavage” is a misnomer, suggesting a brittle-type fracture process which did not occur.

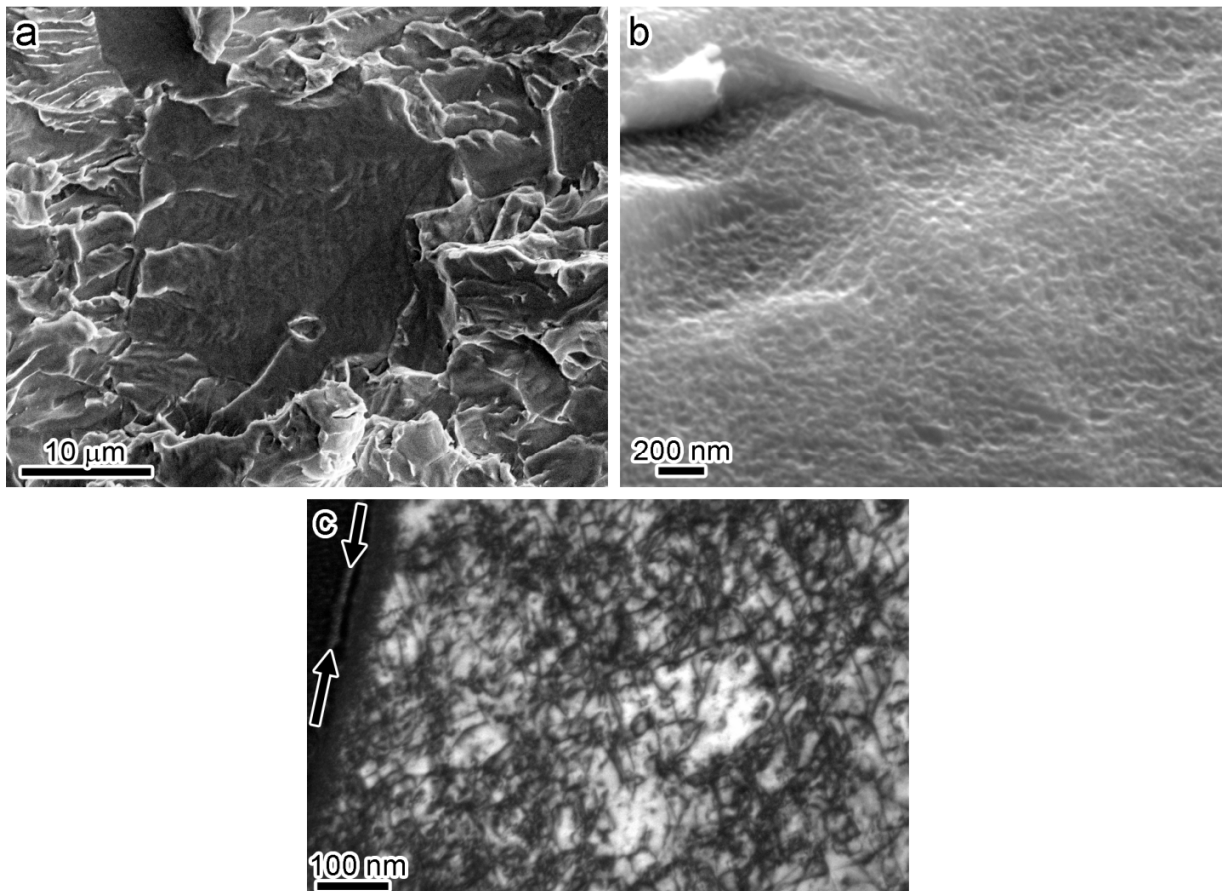


Figure 1. Hydrogen-induced fracture features in ferritic pipeline steel. Compact tension specimens underwent fracture toughness testing in a high pressure hydrogen gas environment. a) SEM micrograph of “Flat” fracture feature typical in this material. b) Higher magnification image of feature tilted at 70° showing the surface curvature and fine features. c) TEM micrograph showing microstructure immediately beneath the fracture surface (marked with arrows) consisting of a high density of dislocations. Adapted from [50].

Additional pieces of information as to which phenomena are active can be garnered by examining other features, such as carbides, in the material. In this particular case, it was found that carbides had little impact on the fracture path, with carbides being found within tens of nanometers of the fracture surface, with no visible perturbation on the fracture surface [50]. Additionally, the interfaces of the carbide were found to be intact, with no evidence of void nucleation, vacancy accumulation, or interface cracking, which would be expected if any of those mechanisms were dominant or even significant to the fracture process.

3.2. Intergranular failure in nickel and iron

Intergranular failure is considered a hallmark of environmental embrittlement [51,52]. Perhaps the most extreme case is the embrittlement of aluminum by liquid gallium, where, given sufficient time for gallium penetration, the fracture toughness can be reduced to virtually zero [53], and the materials crumbles into individual grains. But most cases are less severe, requiring a certain degree of stress, as well as plastic strain before failure. However, the morphology of the fracture surface, along with the rapid failure after the onset of cracking, had led to the conclusion that plasticity is not relevant to the fracture process [54].

Recent work on two model systems, nickel for face-centered cubic [55] and iron for body-centered cubic [56], suggest a different story after looking carefully at the microstructure that develops during the fracture process. Despite the different hydrogen and mechanical loading configurations, both failed intergranularly due to the presence of hydrogen with little evidence of plasticity on the fracture surface (nickel shown in Fig. 2a). The slip traces on the surface would suggest some plasticity, but limited and of a planar character. However, in both cases, dislocation cells were found immediately beneath the fracture surface (Fig. 2b) and the size of the dislocation cells was suggestive of a plastic strain nearly three times what the sample actually experienced macroscopically. In fact, in the nickel case, this dislocation distribution was found to extend to over 3 mm from the fracture surface [57] (Fig. 2c), suggesting that the structures extend throughout the gage length and were formed prior to crack initiation.

It is proposed that hydrogen enhances the plasticity, leading to a dislocation structure in the nickel at 15% strain at failure that would normally only be observed at 40% strain without hydrogen [58]. This amount of plasticity deforms the grain boundaries, weakening them, as well as transports large amounts of hydrogen to the grain boundaries, further lowering their cohesive strength. That this plasticity is crucial for establishing the conditions for enhanced failure is supported by the bulk microstructure away from the fracture surface (Fig. 2c). This microstructure was found to be comprised of dislocation cells with a size larger than those found immediately beneath the fracture surface, but still significantly smaller than expected for the 15% strain at failure, suggesting an acceleration of the plasticity throughout the sample prior to crack initiation.

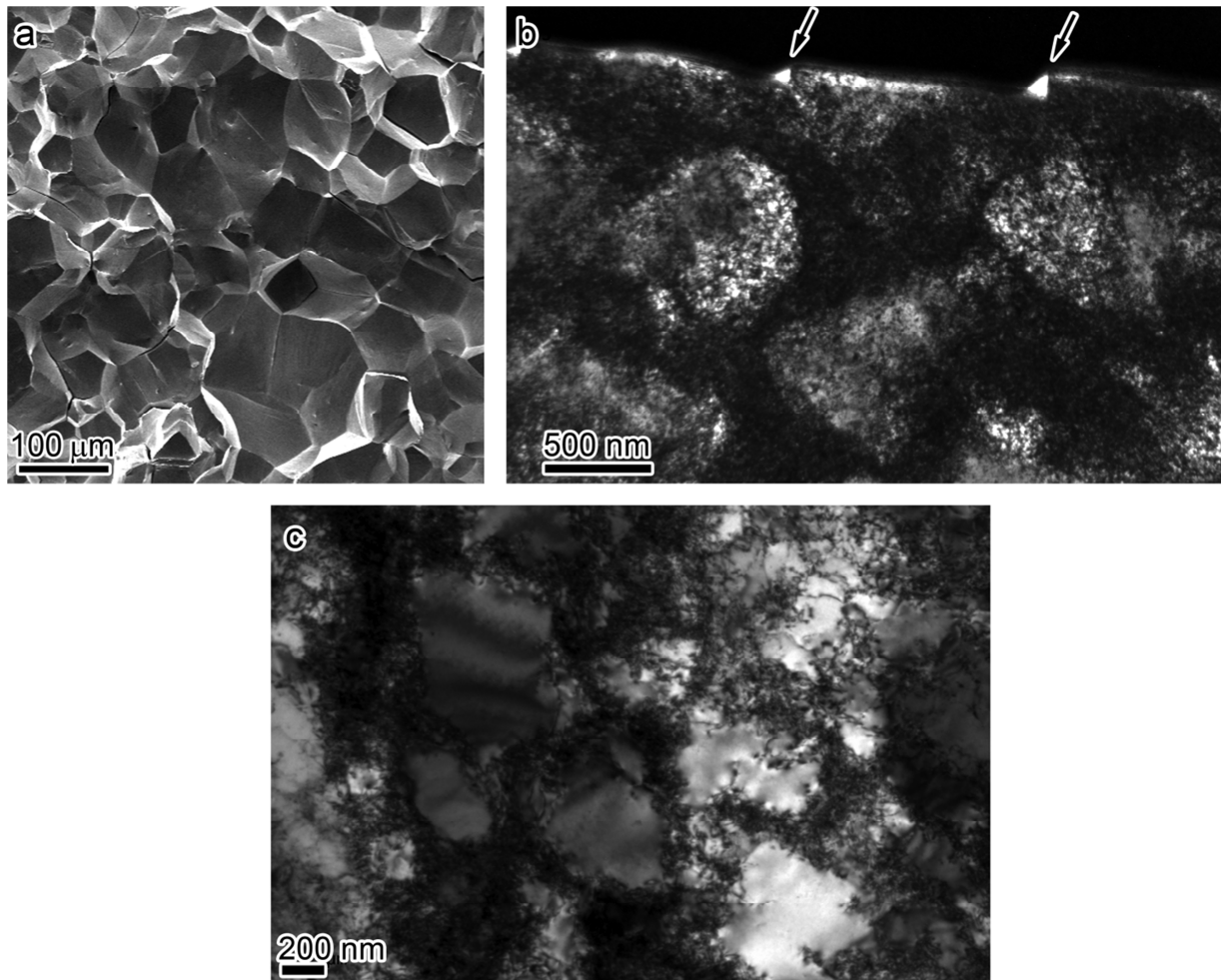


Figure 2. Hydrogen-induced intergranular failure of nickel. Uniaxial tensile tests were conducted on pre-charged tensile bars. a) SEM micrograph showing intergranular failure of fracture surface. b) TEM micrograph showing microstructure immediately underneath the fracture surface, comprising of dislocation cells. Arrows mark steps on the surface, usually labeled as slip traces. c) TEM micrograph showing microstructure 3-6 mm away from the fracture surface (i.e. bulk microstructure after loading). Note that cell structure still remains. Adapted from [55,57].

3.3. Fatigue-crack growth in austenitic stainless steels

Fatigue is a complicated failure mode influenced by many parameters, of which complete mechanistic understanding is still lacking, and many studies are currently on-going to understand the relationship between these parameters, the physical response and the developing microstructure. However, insight into the influence of hydrogen on the microstructure can be gleaned by comparing samples fatigued under identical conditions apart from the absence or presence of hydrogen.

Austenitic stainless steels are usually fairly simple in microstructure (austenite grains), but their deformation can be governed by the development of more complicated microstructural features, such as twinning or deformation-induced martensitic transformations. As an example, 304 stainless steel undergoes a martensitic transformation under loading. This has been observed around the crack tip of an arrested fatigue crack [59]. In that study, it was noted that the presence of hydrogen during fatigue loading resulted in a reduction in large scale martensite formation. In a related study [60], closer examination of the microstructure underneath fatigue fracture surface striations revealed, in the absence of hydrogen, a fine to nano-grained structure of martensite extending several micrometers from the fracture surface (Fig. 3a). The case with hydrogen is quite different (Fig. 3b): a thin layer of nano-grains right at the surface and, below that, an array of sets of thin parallel martensite laths in the austenite matrix. In both cases, fatigue led to a refinement of grains immediately below the fracture surface, though the refinement was more pronounced in the presence of hydrogen. Similarly, there is a refinement in the scale of martensite around the crack in the presence of hydrogen: from a wide band of fine martensite grains around the crack, to a narrower band of thin martensitic laths. A similar refinement in microstructural features with increasing environmental effect was observed under fatigue crack surfaces in 316 stainless steel [60] and in an aluminum alloy [61].

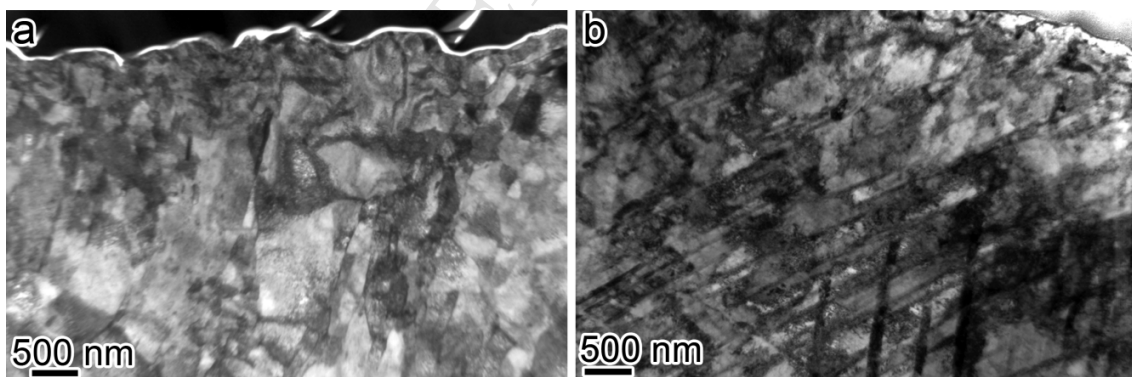


Figure 3. TEM micrographs showing microstructure of 304 stainless steel underneath the fracture surface (top) after fatigue a) in air and b) in hydrogen gas. Adapted from [60].

The results show that, while the microstructural progression in fatigue is quite complicated, there is a clear trend that occurs with the addition of hydrogen: a refinement in feature size and an acceleration of deformation.

3.4. Discussion

As microanalysis tools have progressed, more information about the local behavior of materials in different environments has been discovered. Increasingly, more evidence links hydrogen with the accelerated plasticity. As an example from a different class of metals, the hexagonal phase of titanium (α -titanium) is known for forming hydrides [30,62], but accelerated plasticity has also been observed [30]. More recent studies have shown that plasticity and hydrogen-assisted cracking are critically interlinked: for example, careful examination of a crack tip showed that plasticity was necessary to increase the local hydrogen concentration to levels high enough to promote crack extension [63].

The evidence for hydrogen-enhanced plasticity is strong, as is the connection between accelerated plasticity and fracture. The locally accelerated plasticity can help account for some of the missing pieces of hydrogen embrittlement mechanisms. Hydrogen transport by dislocation motion could redistribute hydrogen into very different concentrations profiles than predicted by Fickian diffusion models [64], potentially leading to high local concentrations and at distances further ahead of the crack tip than in the absence of dislocation transport. The local strain would also disrupt structures and interfaces, and the stress built up at these deformed microstructural features may act as an additional driving force for failure. In summary, the developing microstructure, as influenced by hydrogen, is critical for establishing the conditions for accelerated failure.

4. HELP in martensitic steels

Martensite produced in steel by quenching (often followed by tempering) covers a wide tensile strength range (between 600 MPa and 2 GPa). Lath martensite is a commonly used microstructure in the design of high-strength steels due to its excellent ductility, toughness, workability, and weldability. Accordingly, lath martensitic steels see wide application as the main structural or component members in the construction of ships, buildings, bridges, railroads, pipelines, automobiles, etc. However, it is well known that the presence of hydrogen deteriorates the mechanical properties of lath martensitic steel, which manifests in symptoms such as lower ductility, enhanced fatigue-crack growth rate, and reduced fracture toughness. This hydrogen-induced deterioration of the mechanical properties of lath martensitic steel is often accompanied

by a change in the fracture mode from ductile transgranular to intergranular and “quasi-cleavage” failure. These deleterious effects of hydrogen have motivated numerous studies aiming at understanding the hydrogen embrittlement mechanism in lath martensitic steel [65–75]. Recent results, presented here, suggest that HELP may be the best lens through which to understand the issues pertinent to martensitic steel performance in the presence of hydrogen, and by which to address these issues through optimized materials design.

A middle-carbon ultra-high strength tempered lath martensitic steel was prepared and four-point bend tests were conducted under three conditions: in the absence of hydrogen at room temperature; in the absence of hydrogen at low temperature ($\approx -150^{\circ}\text{C}/123\text{K}$); and in the presence of hydrogen at room temperature [76]. The hydrogen-charged specimen was pre-charged with hydrogen in a high-pressure gaseous hydrogen environment prior to the bend test. The thermal charging introduced a nominal hydrogen content of 0.57 mass ppm (31.7 at ppm).

Hydrogen reduced the maximum nominal bending stress from 2415 to 501 MPa at room temperature, a decrease of nearly a factor of 5. The sample tested at -150°C showed only a small change (from 2415 to 2310 MPa) in the maximum nominal bending stress, followed by an abrupt drop in stress indicating brittle failure.

At room temperature and in the absence of hydrogen, the fracture was primarily by ductile microvoid coalescence. However, the fracture surface generated in the presence of hydrogen had “flat” and “quasi-cleavage” features with some evidence of small-scale ductile processes (see Fig. 4a and b, respectively). At low temperature, the fracture surface generated in the absence of hydrogen was dominated by a “cleavage-like” morphology, which is also often referred to as “quasi-cleavage” (see Fig. 4c) [77]. The “brittle” fracture surfaces generated in the absence and presence of hydrogen showed similarities despite the significant differences in their fracture load. Both were decorated with fine, lath-like features that were comparable in dimension to the martensite laths in the starting material.

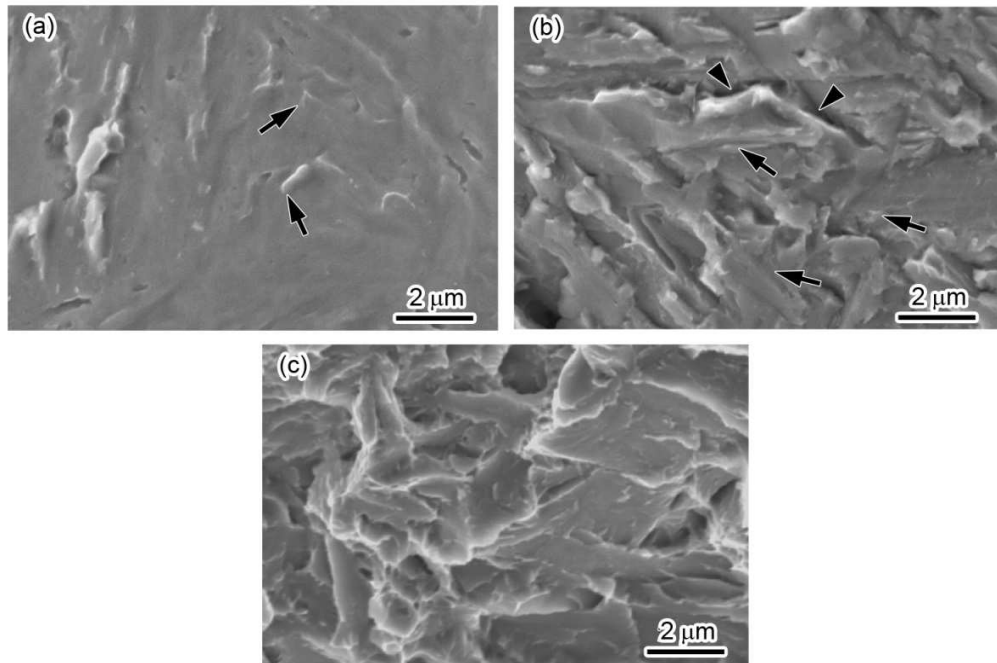


Figure 4. SEM images of fracture surfaces of ruptured four-point bend specimens of a lath martensitic steel: (a) hydrogen-induced “flat” feature produced at room temperature; (b) hydrogen-induced “quasi-cleavage” feature produced at room temperature; (c) low-temperature induced “quasi-cleavage” feature in the absence of hydrogen. Arrows in (a) indicate fine tear ridges. Arrows and arrowheads in (b) show fine serrated markings and secondary cracks, respectively. [76]

Differences in the fracture paths associated with these three types of fracture surfaces were determined by examining sections of the fracture surface and the microstructure underneath [76]. For the “flat” surface (Fig. 5a), the fracture path was clearly along prior austenite grain boundaries denoting intergranular fracture. In contrast, the fracture path for hydrogen-induced “quasi-cleavage” surfaces was consistent with being along the {110} slip plane, the lath habit plane. Other studies of “quasi-cleavage” features in lath martensitic steels confirm failure along the {110} plane [78,79]. This fracture path corresponds to failure along lath/block boundaries with translath steps (Fig. 5b). In both cases, intense slip bands (deformation bands) were observed altering the lath boundaries. Similar fracture features were observed in several ultra-high strength martensitic steels, and were interpreted following the same fracture path and as having been formed by a similar mechanism [80]. In contrast to hydrogen-induced fracture surfaces, the low temperature fracture “quasi-cleavage” path (Fig. 5c) was observed to be {100}

plane cleavage, and, as expected for true brittle failure, there was no significant change in the microstructure compared to before deformation.

The degree of hydrogen-induced intergranular and “quasi-cleavage” fracture features in lath martensitic steel depend upon many factors, including the strength of the steel, the hydrogen content, and the charging conditions [5]. In general, a larger percentage of the fracture surface will be comprised of these features with increasing steel strength and increasing hydrogen content. It has been shown that intergranular failure tends to propagate suddenly, while “quasi-cleavage” fracture follows more gradually [81], suggesting that understanding the difference and controlling for the process may lead to increased hydrogen resistance. Figures 6a and c show the TEM bright-field micrographs of the microstructure immediately beneath the intergranular fracture surface and the “quasi-cleavage” fracture surface, respectively. In Figs. 6a and c, arrows and arrowheads show, respectively, the slip bands and discernible lath boundaries. The tracings of Figs. 6a and c are shown in Figs. 6b and d for clarity. There is a distinct difference between the microstructure underneath the two fracture surfaces with regard to the directions of activated slip systems relative to the lath structures. As shown in Figs. 6a and b, beneath the intergranular fracture surface, slip bands are approximately parallel to the lath boundaries and they are inclined to the prior austenite grain boundary. On the other hand, beneath the “quasi-cleavage” fracture surface, slip bands are inclined to the lath boundaries and intersect with the fracture surface, Figs. 6c and d. Which type of boundary fails (lath/block or prior austenite grain) appears to be dependent upon which slip systems were most active and which boundary the resulting slip bands intersect, as determined by local constraint and microstructure. Controlling features such as prior austenite grain size and martensite packet/block size may allow control of the degree of intergranular failure and improve mechanical performance in a hydrogen environment [80].

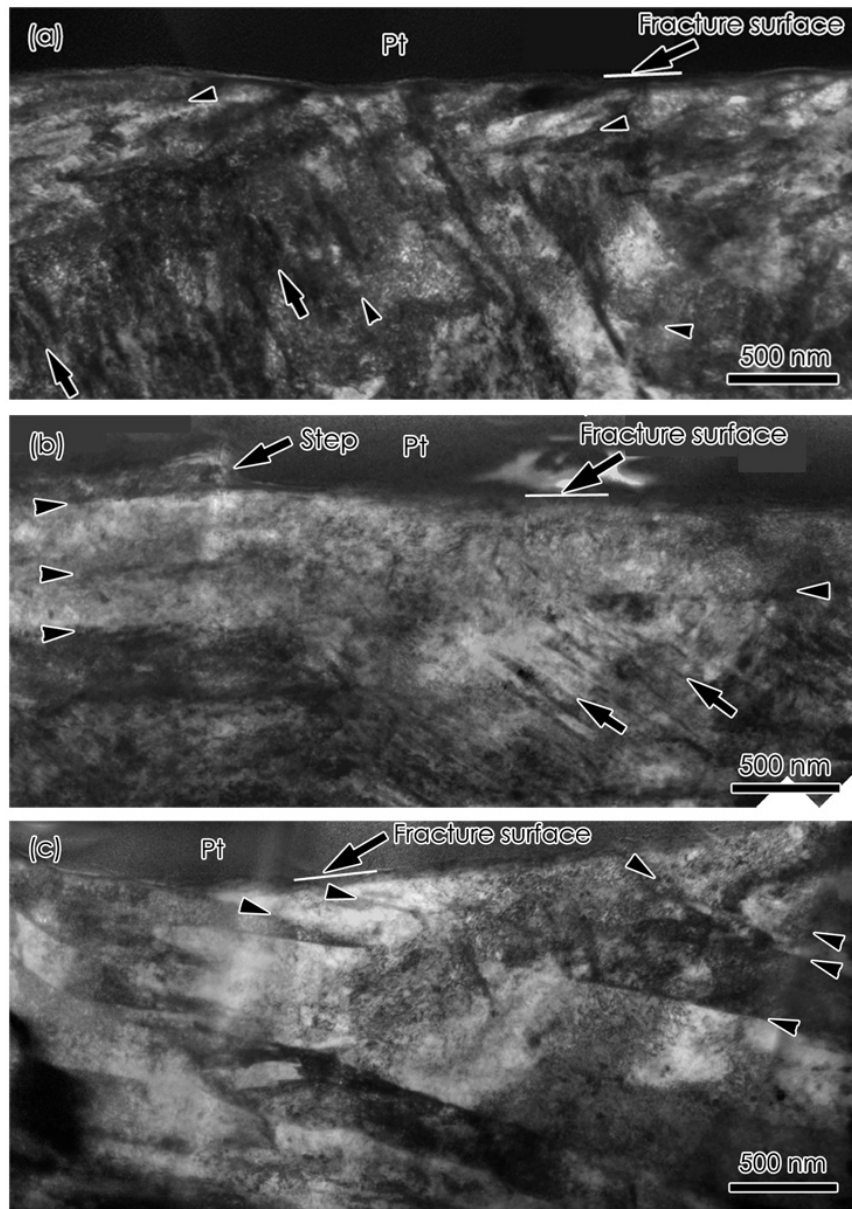


Figure 5. TEM bright-field micrographs showing microstructure immediately under fracture surfaces of ruptured four-point bend specimens of a lath martensitic steel: (a) under a hydrogen-induced “flat” fracture surface produced at room temperature; (b) under a hydrogen-induced “quasi-cleavage” fracture surface produced at room temperature; (c) under a “quasi-cleavage” fracture surface produced at low temperature. Arrows and arrowheads indicate slip bands and lath boundaries, respectively. [76]

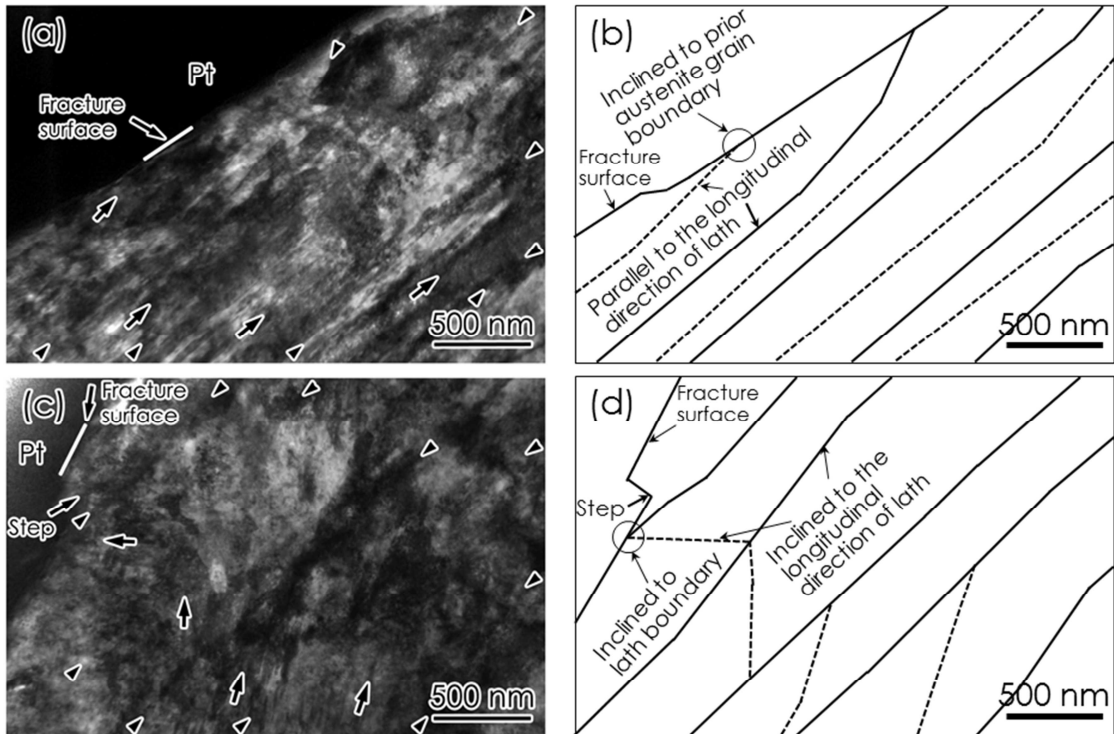


Figure 6. TEM bright-field micrographs and tracings showing microstructure immediately under hydrogen-induced intergranular (a, b); and “quasi-cleavage” fracture surfaces (c, d). Arrows and arrowheads in (a, c) indicate slip bands and lath boundaries, respectively. Dashed lines indicate slip bands and solid lines denote lath boundaries in (b, d). [82]

Hydrogen microprint technique [83], in which AgBr is reduced to Ag by hydrogen, was used to visualize hydrogen distribution on hydrogen-induced fracture surfaces [82]. Hydrogen accumulation was observed close to the prior austenite grain boundary on a “quasi-cleavage” fracture surface, consistent with hydrogen transport to boundaries by dislocation activity. High angle boundaries such as prior austenite grain boundaries, packet and block boundaries can create dislocation pile-ups at the boundaries by hindering the dislocation movement which results in a greater local hydrogen accumulation near the boundaries.

An increase in dislocation processes in the presence of hydrogen was evident from the partial destruction of the lath/block boundaries observed beneath the fracture surfaces. Moreover, the extensive depth of the dislocation activity suggests that the evolved microstructure existed prior to crack advance, and was not a consequence of an advancing crack. It is rationalized that HELP

led to an increase in the dislocation density and activity close to the boundaries, which resulted in modification of the boundary structures [76]. Increased dislocation density hardens the matrix, raises the local stress, and increases hydrogen concentration at the boundaries which, consequently, reduces the cohesive energy of the boundaries. Fracture along the boundaries is the result. Intergranular failure results when slip systems intersect prior austenite grain boundaries that have been weakened by the locally accumulated hydrogen and “quasi-cleavage” occurs when they intersect block boundaries of which cohesive strength has been reduced by hydrogen. The interaction of slip systems with the different boundary types, the change in the energetics of the boundaries due to the slip transfer process, and the accumulated hydrogen should determine which boundaries fail. Thus, similarly to the boundary failures discussed in Section 3.2, both hydrogen-induced fracture surface morphologies in lath martensitic steel were driven by a hydrogen-enhanced and plasticity-mediated decohesion mechanism.

5. HELP in austenitic steels

Austenitic steels are widely utilized for industrial purposes such as component members in automobiles, off-shore oil rigs, as well as for surgical instruments and other specialized parts. It is a wide-encompassing material group, including alloy families like stainless steels (AISI 304, 310S, 316, 316L, etc.), heat-resistant steels (JIS SUH310, SUH660, etc.) and high manganese steels (transformation-induced plasticity steel, twinning-induced plasticity steel, etc.). Austenitic stainless steels are generally considered better for hydrogen service [84], as the face-centered cubic structure of austenite leads to significantly slower uptake of hydrogen. Under certain conditions, austenite can transform to martensite at low temperature or by deformation, but this generally depends on factors such as chemical composition, and even an alloy labeled as “stable” may still exhibit some degree of transformation to martensite.

Despite the improvement in performance compared to most ferritic and martensitic steels, the presence of hydrogen still results in a reduction in the mechanical performance of austenitic steels, and this deterioration manifests as decreased elongation, enhanced fatigue-crack growth rate, and reduced fracture toughness, analogously to in other susceptible materials. Metastable austenitic steels in particular show high susceptibility to hydrogen embrittlement, where the transformation to martensite can make the hydrogen-induced failure mechanism of austenitic

steels rather complicated. Despite numerous studies focusing on elucidating the hydrogen embrittlement mechanism of austenitic steels [84–90], the mechanism is still not clearly understood.

5.1. Differences between austenitic and ferritic steels pertaining to the hydrogen effect

The face-centered cubic structure of austenite leads to certain differences in behavior, especially as regards the hydrogen effect. Due to the differences in crystal structure, the binding energy, size, and nearest-neighbor distances of hydrogen interstitial sites in austenite are different from in ferrite, and, consequently, the diffusivity of hydrogen in the austenitic matrix is significantly lower compared to that in body-centered cubic ferritic materials, by as much as 5 orders of magnitude [91]. This has an impact on how these materials can be tested for hydrogen effect: a slow strain rate is needed to allow time for sufficient hydrogen accumulation in the material from the gas environment to occur, but the lowest practical strain rates for tensile tests may still be too fast. The consequence is that most room temperature tensile tests of austenitic steels in hydrogen atmosphere will not show an effect of hydrogen on the mechanical properties [92], though pre-cracked or fatigued specimens will [84]. Techniques such as pre-charging in a higher temperature hydrogen environment are typically employed to overcome this problem, though, if not correctly done, hydrogen effects will be limited to a thin surface layer.

Due to the nature of austenite (thermodynamically a high temperature phase), the microstructure of “austenitic” steels can be complex, ranging from 100% austenite grains to mixtures of austenite grains with ferrite, ε -martensite (hexagonal cubic packed phase), or α' -martensite grains, depending upon processing of the material. For example, upon cooling, austenitic welds can become a duplex structure containing austenite and ferrite grains [93]. In a duplex material, differences in hydrogen-influenced behavior can be expected: the ferrite phase acts as a fast pathway for hydrogen diffusion through the material, and differences in mechanical response of the two different phases can be exacerbated by the HELP effect. It was found that the resistance to hydrogen fracture of duplex austenite/ferrite microstructures tended to decrease with increasing ferrite content [94]. Additionally, as mentioned earlier, martensitic phases can form during deformation, and their formation is thought detrimental, with improved austenite stability, and factors contributing to it, such as increased nickel content, being associated with improved hydrogen performance [92].

There is a variety of deformation modes available in austenitic stainless steels: dislocation glide, mechanical twinning, and martensitic transformation. Which deformation mode is dominant depends on the stacking fault energy (SFE) of the material: displacement transformations to ϵ -martensite occurring with low SFE, dislocation glide occurring with high SFE, and mechanical twinning dominating in the intermediate regime [95]. Hydrogen effects, such as HELP processes, will almost certainly still impact these processes. Hydrogen has a tendency to induce phase transformations from austenite to either ϵ - or α' martensite [96]. As for twinning, nitrogen, which is known to decrease SFE, tends to lower the strain for the onset of deformation twinning [97], suggesting that hydrogen could also have a similar effect. In fact, TEM studies found that hydrogen caused a 19% reduction in the SFE of a 310S stainless steel [32], which may be sufficient to alter the dominant deformation mode. It is important to note that twinning and strain-induced martensitic transformations occur through the action of successive partial dislocations. Observations show that the presence of hydrogen tends to lead to thinner twins during deformation, by enhancing planar slip [94,98]. Hydrogen impacts the mobility of perfect and partial dislocations [43], and austenitic steels are not an exception to the observation of increased mobility [99,100].

While which deformation mode is dominant will evidently affect the austenitic steel's performance in a hydrogen environment, it was found that hydrogen susceptibility is not correlated with SFE [101], suggesting that hydrogen embrittlement is not necessarily dependent on the deformation mode. However, there does seem to be a general trend in susceptibility that correlates with austenite stability [102–104], as shown in Figure 7. Figure 7 compares the performance of various austenitic steels in helium and in hydrogen, with a lower relative reduction in area (ratio of the reduction in area in hydrogen to the reduction in helium) shown in tensile testing indicating poorer performance in hydrogen [104]. As the stability of austenite generally rates as 310S as the most stable, then 316, then 304 as the least stable of the three, there is a clear decrease in hydrogen performance with decreasing stability. However, there is a lack of direct evidence that the transformation to martensite is critical to the degradation of ductility in hydrogen [84]. It is also notable that Figure 7 also clearly demonstrates that there is a specific temperature range in which hydrogen embrittlement occurs. The greatest embrittlement occurs at temperatures below room temperature for these austenitic stainless steels, and that is

thought to be due to the lowering of the SFE with temperature, leading to more localized deformation [105], and therefore exacerbating the HELP effect.

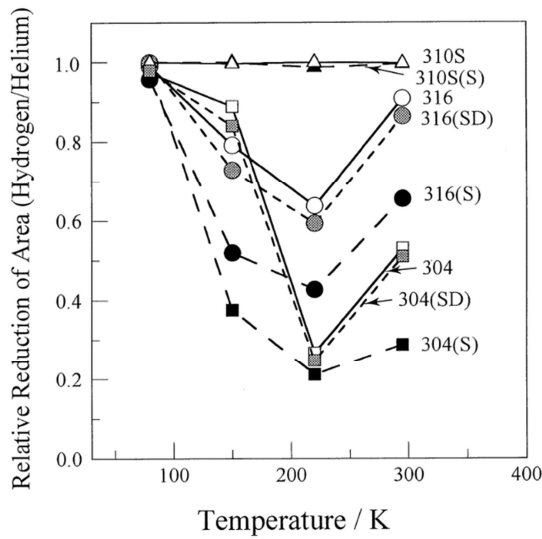


Figure 7. The relative reduction of area for 304, 310S and 316 austenitic stainless steels tensioned in 1 MPa hydrogen versus 1 MPa helium gas as a function of testing temperature. S and SD indicate sensitized and desensitized heat treatments, respectively [104]. Sensitization affects the number of grain boundary carbides, which, acting as additional hydrogen trapping sites and crack nucleation sites, can affect hydrogen susceptibility.

5.2. Hydrogen-induced failure in austenitic steels

Hydrogen can have a wide-range of effects on the fracture of austenitic steels, depending upon the alloy and the hydrogen loading conditions. As several alloys, especially those stable with respect to austenite-to-martensite transformations, are considered resistant to hydrogen, one would expect little to no change in their mechanical behavior or the ductile fracture mode due to the presence of hydrogen. In 316L steel, similar-sized dimple failure was observed in both the hydrogen-charged and uncharged samples, and accordingly, no difference in the deformation behavior was observed [102]. In other studies [92], though the failure mode remained ductile, a shift to smaller average dimple sizes was observed, which was attributed to an increased number of void nucleation events. Hydrogen was proposed to have two impacts on void nucleation: decrease in the strength of the particle/matrix interface, and increased slip localization leading to dense slip bands impinging on particles and generating higher stresses than if the deformation were more homogeneous.

In some alloys and conditions, the presence of hydrogen results in the elongation of the voids on the fracture surface [98,105,106], often associated with a drop in fracture toughness. This is still a ductile failure, but instead of nucleating the voids at locations (such as inclusions), these voids initiate at the intersection of deformation bands with other deformation bands or grain boundaries [98,107]. This transition becomes more obvious when comparing samples of 304L/308L weld metals fractured in the presence of hydrogen at room temperature and at 223K (-50°C) [105], where the lower temperature is thought to exacerbate the localized deformation by decreasing the SFE, generating thinner deformation twins, and altering the free-energy differences between the different phases.

When hydrogen-induced deformation bands intersect grain boundaries, they may create voids along the grain boundary. The presence of a critical number of voids may sufficiently weaken the boundary such that intergranular failure occurs [107–109].

High coherence twin boundaries (low- Σ boundaries) are known for their resistance to intergranular failure. Several studies have shown that increasing the number of strong low- Σ boundaries (such as $\Sigma 3$ twin boundaries) to a material can reduce the tendency for intergranular failure [110,111]. In addition to their strength, it is thought that their coherency would make them poor hydrogen traps. However, in the presence of hydrogen, cracking along these boundaries has been found in certain austenitic steels [90,109,112], resulting in flat features on the fracture surface, particularly in a class of steels dubbed TWIP (twinning induced plasticity) steels, wherein, as the name suggests, the principal deformation mode is twinning. In TWIP steels, cracks formed in the presence of hydrogen propagated primarily along grain boundaries and deformation twin boundaries, while initiation occurred at grain boundary triple junctions or twin/twin intersections [112]. Deformation twin intersections can be the site of microcracking even in the absence of environmental effects [97]. Twin lamella act as efficient obstacles, preventing further twin propagation, with the result that high internal stresses are built up at these intersections. And elements which decrease the stacking fault energy (such as hydrogen) increase the ductile-to-brittle-transition temperature due to this behavior. In a single-crystal test, cracking occurred along deformation-induced twins in the presence of hydrogen [113]. These stress concentrators can also cause the cracking of nearby boundaries [112]. It is proposed that a combination of these high stress concentrations, located at the tips of deformation twins

intersecting obstacle twins, and the local disturbance of the obstacle twin boundary coherency by dislocation activity can lead to cracking along these supposedly strong low- Σ boundaries [112].

Martensitic transformations near grain boundaries can also lead to twin boundary failure [114]. Martensite clusters intersecting a twin boundary create a zigzag phase boundary in place of the originally straight twin boundary line. Due to the formation of martensite on either side of the boundary, it was typical for the distribution of martensite to be different, leading to sections of boundary with martensite on one side and austenite on the other. Due to the difference in hydrogen diffusivity and solubility in martensite and austenite, it was proposed that hydrogen accumulation would occur at these boundaries. The combination of the high stress, high hydrogen concentration and brittle phases leads to boundary failure.

In duplex steels, “quasi-cleavage” features tend to combine with ductile tearing to form what appear to be elongated void failures. These “quasi-cleavage” features are due to failure through the ferrite phase, which appears to be due to cleavage-like processes, initiated by stress concentrations at the ferrite/austenite boundary from enhanced plasticity in the austenite phase [93,106,107]. Alternatively, the deformation in the austenite can promote cracking along the ferrite/austenite interface [93,94], in a similar process to those described above with austenite/martensite interfaces.

5.3. Discussion

Based on the above examples, it is clear that the HELP mechanism operates in the hydrogen-induced failure process of austenitic stainless steels. Whether the fracture features were ductile, brittle transgranular, or boundary failure, they all were associated with enhanced localized plasticity, whether in the form of planar dislocation slip, twinning or martensitic transformations. In fact, in a study looking at the effects of stabilizing the austenite, it was found that the best performance was not by a steel that was composed of completely stable austenite, it was a steel with initially 100% austenite and limited transformation to stable ϵ -martensite during deformation [103]. It is proposed that by controlling the plasticity in the form of martensitic transformations, where the trailing partial dislocation is stationary, and avoiding dislocation slip, some of the HELP effects can be suppressed, leading to improved hydrogen performance.

The factors that control which deformation and failure processes will be dominant are still unclear. For example, whereas the martensite intersecting twin boundaries is the primary cause of failure in one case [114], in another case, while present along deformation bands in the vicinity of cracks in the duplex steel [94], it does not appear to impact the failure. In fact, hydrogen's impact on the martensitic transformation is still unknown. This is a broad field, still requiring additional study, but it is clear that understanding the deformation processes is a crucial piece.

6. Atomistic modeling of the underlying principles of HELP mechanism

Hydrogen is notoriously tricky to detect by certain experimental techniques, and certain measurements (with or without hydrogen) are not yet possible to achieve, especially at the atomic scale. Correspondingly, there is still information that is lacking in order to have a full understanding of hydrogen-metals interactions. This gap can be addressed through atomistic modeling. It is important to note that there are certain systematic issues with atomistic models: calculations are generally conducted at or close to a temperature of 0 K, and, due to computation time costs, time scales in a dynamic simulation are typically short, resulting in issues such as extremely high strain rates. This is worth noting because hydrogen embrittlement is sensitive to temperature and strain rate, and is known to not occur at low temperatures and high strain rates. In spite of these drawbacks, however, useful information can still be gleaned from atomistic simulations. In the following, atomistic simulations of some of the underlying features of the HELP mechanism are reviewed along with their impacts on the understanding of the mechanism.

6.1. Hydrogen-modified dislocation mobility in steels

The hydrogen's influence on dislocation mobility is the cornerstone of the HELP mechanism, and yet the underlying mechanism at the atomic scale for why it occurs is still not well understood. Atomistic modeling of hydrogen-dislocation and dislocation-dislocation interactions in the presence of hydrogen can provide valuable insight into the mechanism.

Supporting mechanisms for the elastic shielding effect of hydrogen were established by addressing atomistic interaction of hydrogen atoms with dislocations. By using *ab initio* calculations, Lu et al. demonstrated hydrogen-enhanced individual dislocation motion in aluminum at the atomic scale [37]. They argued that a plausible explanation of HELP should

consider the hydrogen atoms trapped in the dislocation core area as well. They found that hydrogen at the dislocation core in aluminum can reduce the dislocation line energy, modify the dislocation core structure, and decrease the Peierls stresses of edge, screw and mixed dislocations by more than one order of magnitude. However, given the already low Peierls stress of a dislocation in aluminum, it is arguable whether this would have a significant impact on behavior. The reduction of Peierls stress and dislocation line energy have also been shown on individual edge [115] and screw dislocations [116] of α -iron by molecular dynamic (MD) studies with density functional theory (DFT)-based empirical potentials. Another series of DFT, MD, and elastic line tension calculations has revealed that hydrogen atoms trapped in the dislocation core area can also facilitate the formation of screw dislocation kink-pairs in α -iron, in a limited temperature range, by lowering the kink nucleation energy [38,116–118], thus enhancing the mobility of dislocations. Accounting for local hydrogen-hydrogen interactions in the hydrogen atmosphere surrounding the dislocation results in an amplification of the elastic shielding effect in simulations [119].

It is important to note that besides the influence on individual dislocation motion, the hydrogen-induced shielding effect on the dislocation elastic stress field can also reduce the interaction energy of dislocations with other obstacles, resulting in the easy multiplication of dislocations and highly-developed dislocation structures. MD simulations on α -iron nanocrystals found that hydrogen increased dislocation density by 25% at a strain of 10% in uniaxial tension, and changed the deformation morphology from discrete slip in the absence of hydrogen to homogeneous in its presence [120]. However, the approaches of MD simulations remain limited at describing large scale dislocation-dislocation and dislocation-hydrogen interactions due to the unavailability of sufficiently accurate metal-hydrogen and metal-metal interatomic potentials to properly describe dislocation motion [121,122]. Other limitations of the MD models include the limited volume that can be modeled, resulting in a small number of dislocations included, and a possibly unphysically small equilibrium distance in their spacing (less than the 40-120 nm distances measured in TEM studies [9]). There is a scarcity of *ab initio* studies on the mutual interactions of dislocations and on dislocation-barrier interactions. Further study on this issue requires improvements in accuracy and efficiency of the empirical potential and calculation methods.

6.2. Hydrogen induced slip planarity

In face-centered cubic crystal systems, hydrogen induced slip planarity can promote the transformation of homogeneous macroscopic plastic deformation into intense shear. When the slip behavior is dominated by planar slip, because the Peierls energy barrier for the edge partial dislocation is much lower than a perfect screw dislocation, the deformation process can evolve at lower stress levels. There are two viable explanations for hydrogen induced slip planarity. The first considers that hydrogen-reduced stacking fault energy will result in an increase of the equilibrium separation distance between two edge partials, and thus prevent constriction, a critical step for cross-slip to occur [28,123,124]. However, in an MD simulation of the Ni-H system, the trapping energy of hydrogen at a stacking fault was calculated to only be 0.075 eV, compared to 0.1-0.3 eV for dislocations [125,126], so, it is unlikely that hydrogen would have a significant effect on the separation distance by the lowering of the stacking fault energy. Experimental results revealed that the reduction of stacking fault energy is at most 20% in austenitic stainless steel [32] and 35% in Ni [124], though the importance of this reduction is under debate since *ab initio* calculations have shown that dissociation behavior was stable even with 40% reduction of stacking fault energy [37]. The open question remains on whether the magnitude of reduction on stacking fault energy is sufficient for an increase in slip planarity. Another explanation for slip planarity is based on the energetic comparison that the binding energy of hydrogen to an edge partial dislocation is higher than that to a perfect screw dislocation [10,19,90]. For instance, the binding energy of hydrogen to edge dislocations in aluminum is twice of that of screw dislocations [37]. Therefore, the constriction process for cross-slip of screw dislocations requires extra energy consumption to “pump” hydrogen atoms out of the energy wells of edge dislocations to allow them to reorient to screw-type. Additionally, the latter explanation suggests that the attractive interaction of the edge partial dislocations can be decreased by hydrogen shielding effect which will also result in an increase in the separation distance and the work required for constriction, and therefore will encourage planar slip behavior.

6.3. Hydrogen-enhanced dislocation motion and fracture mechanics

Because of the limited capability of current atomistic simulations in spanning the diffusion time-scales in most metals, it is difficult to mimic the hydrogen transport behavior along with

dislocation motion, especially at the intermediate/high plastic strain level before the failure event. The evaluation of all essential factors in hydrogen-related dynamic crack propagation behavior still remains a challenge in current state-of-the-art modelling approaches. To simplify the problem, different aspects, for instance, the effects of local hydrogen concentration, dislocation emission behavior, and modification of local atomic configurations, have been studied separately. However, it is noteworthy that none of these models directly account for the dynamic hydrogen-dislocation interactions and hydrogen transport by dislocations, which are envisaged as key factors for linking hydrogen-enhanced plasticity with a fracture mechanism.

Most of the simulations on crack behavior in the presence of hydrogen focused on the intergranular fracture mode, since it is representative of the hydrogen-induced ductile-to-brittle transition in most metals. To evaluate the role of plasticity processes, one important question is whether the hydrogen-induced reduction of the grain boundary cohesive energy by itself can induce intergranular fracture. By applying the classic Gibbs adsorption isotherm to the separation process of grain boundaries, the Hirth-Rice model [127] and, subsequently, the Rice-Wang model [128] suggest that whether a segregant has a strengthening or embrittling effect on a grain boundary is strongly dependent on its segregation energy to the grain boundary (GB) and to the separated free surfaces (FS). That is, if trapping sites on FS are energetically more favorable by the segregant atoms than the trapping sites on GB, the crack under external stress is expected to propagate along GB. The embrittlement potency was defined as the difference between the segregation energy on GB and on FS ($\Delta E_{em} = E_{GB}^{seg} - E_{FS}^{seg}$) by Freeman and co-workers [129–135]. They stated that, if a segregant has $\Delta E_{em} > 0$, it is a potential embrittler and may induce intergranular fracture.

The Rice-Wang model has been successfully applied to identify the embrittling and strengthening effect of different atom species in α -Fe and Ni [134]. Using the Rice-Wang model and experimentally-derived segregation energies for H atoms in α -Fe, Anderson et al. [136] predicted that the ideal work of separation can be decreased by 56% at 0.01 atm hydrogen gas pressure, in which hydrogen coverage was assumed to be around 16 nm^{-2} . Zhang et al. [133] calculated the embrittlement potency of hydrogen on a $\Sigma 3(111)$ boundary in α -Fe as +0.26 eV through first principle calculations, while Yamaguchi et al. [137,138] found the potency as +0.34 eV with a 60 – 70% reduction in the ideal work of separation using a similar approach. As noted

in Rice and Wang's work [128], there is no unique value of segregation energy, as the energy depends on the trapping site and the type of grain boundary. The generated surface energy may also influence the likelihood of grain boundary fracture. For example, Kirchheim et al. applied this notion to explain why some coherent twin boundaries may fail preferentially due to the presence of hydrogen, despite the lower energy of twin boundaries compared to general grain boundaries: a (111)-oriented fracture surface has the smallest surface energy and the largest hydrogen coverage, making it more energetically favorable than the result of separating a general grain boundary [139]. By applying molecular statics calculations to <100> tilt boundaries in α -Fe, Solanki et al. [140] found that the hydrogen segregation energy in different trap sites strongly depends on the local atomic GB structure.

It is not always the case that positive embrittlement potency should be related to embrittlement and intergranular failure. For instance, Yuasa et al. [141] calculated the embrittlement potency in the Mg-H system as +0.19 eV, but they obtained a strengthening effect from a first-principles computational tensile test; they attributed the experimentally observed intergranular fracture to hydrogen-suppressed dislocation emission from grain boundaries. Although the calculated positive embrittlement potency in the α -Fe-H system predicted a likelihood of intergranular failure, experiments have shown that the predominant failure mode of α -Fe in high pressure hydrogen gas is transgranular [142], and that hydrogen-induced intergranular fracture is only found for cases with severe cathodic charging [56,143,144]. Therefore, in order to evaluate the importance of ideal work of separation in controlling hydrogen-induced fracture behavior, the geometrical effect of different trapping sites and the environmental effect on H excesses (coverages) need to be addressed.

Wang et al. [145,146] applied a molecular statics calculation with a DFT-based empirical potential to probe the trapping states of hydrogen in 50 types of <100> symmetric tilt boundaries and 50 types of <110> symmetric tilt boundaries with different misorientation angles in α -Fe. The effect of environment, i.e., the fugacity/pressure of hydrogen, on the local hydrogen excess was considered by modifying the chemical potential of hydrogen in the system and linking the chemical potential to hydrogen pressure through thermodynamic equations [147]. Their studies showed that the cohesive energy of grain boundary decreases precipitously even with low hydrogen gas pressure, but the reduction is much less than that predicted by Anderson et al. [136]

and Yamaguchi et al. [137,138].

Figure 8 illustrates two examples of the effect of hydrogen pressure on grain boundary cohesive energy, i.e. the ideal work of separation for the fracture process. The horizontal dashed lines indicate the ideal work of separation without hydrogen, and the solid lines denote the work with hydrogen by assuming that all trapping sites with segregation energy lower than an octahedral lattice site are available to hydrogen atoms. In the $\Sigma 3(111)GB-(111)FS$ system, Fig. 8a, the ideal work of separation in hydrogen $2\gamma_{int}^H$ is decreased by 10% at 1 atm and by 20% at 1000 atm. For $\Sigma 5(120)GB-(120)FS$ case, Fig. 8b, the reduction is 18% at 1 atm and 32% at 1000 atm. In both cases, there is a rapid drop in the cohesive energy after the introduction of hydrogen, and then the decrease rate is very slow at pressures higher than 1000 atm. By comparing the 100 different boundary types investigated, Wang et al. concluded that the magnitude of the reduction in the cohesive energy is strongly dependent on the grain boundary type. Moreover, they demonstrated that estimating the decrease of cohesive energy by using embrittlement potency always overestimates the H decohesion effect on the ideal GB work of separation (horizontal solid lines in Fig. 8); compare the calculated reduction of 70% by Yamaguchi et al. [137,138] with the 32% reduction calculated in this study by Wang et al.

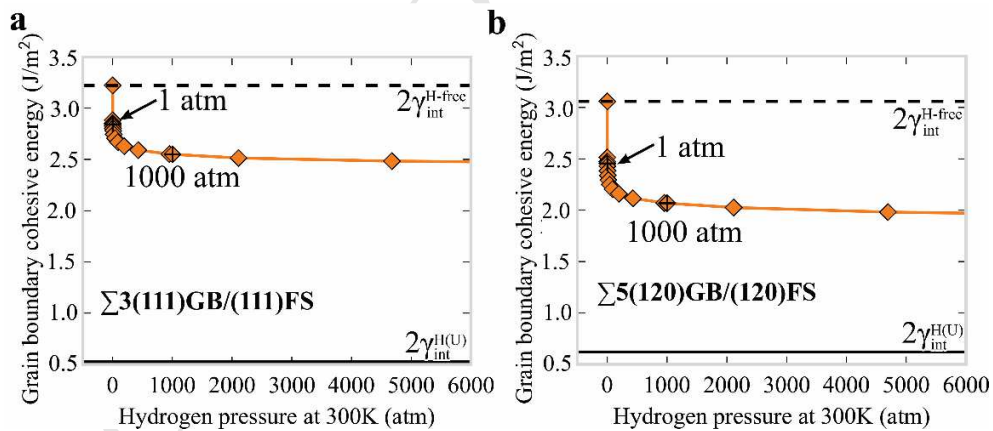


Figure 8. The ideal work of separation for (a) $\Sigma 3(111)GB$ and (b) $\Sigma 5(120)GB$ at different hydrogen gas pressures in α -Fe. Adapted from [145,146]. The horizontal dashed lines indicate the work without hydrogen, and the solid lines indicate the work predicted by assuming all trapping sites available.

This potentially insufficient decrease in grain boundary cohesive energy leads to the question of what other factors hydrogen can influence to cause intergranular failure. One reason invoked

for the change in fracture mode is the modification of the local atomic configurations around the crack path by dislocation emission and dislocation interactions with other defects [148]. Taketomi et al. [149] investigated the effect of hydrogen on the emission of a $\{112\}<111>$ edge dislocation from a mode II crack tip in α -Fe using MD simulations, and found that the hydrogen-enhanced dislocation emission is proportional to the hydrogen content around the crack tip. They attributed this result to a linear reduction of stacking fault energy induced by hydrogen. It should be mentioned that in opposition to Taketomi et al.'s result, Song and Curtin [150], using a different empirical potential, reported a suppression effect of hydrogen on the dislocation emission during loading of a mode I crack tip in the α -Fe system. Such a discrepancy could be caused by either the accuracy of the empirical potential or the different method for loading the system. The fact that these discrepancies exist demonstrate how necessary it is to use proper empirical potentials and algorithms for handling the dislocation-hydrogen dynamic interactions in order to correctly predict the behavior at the atomic scale. Using the approach of virtual strain-controlled tensile deformation in a MD calculation, Kuhr et al. [151] investigated the mechanical response of a Ni polycrystalline model with randomly generated grain boundaries with hydrogen coverage of up to 8 H-atoms/nm². They found that increased hydrogen concentration on the grain boundary produces more disordered structures in the boundary. These structures have extra free volume for accommodating hydrogen atoms and facilitate the emission of Shockley partial dislocations from these sites. As a result, the number of dislocations in pile-ups at grain boundaries was increased by hydrogen, and significant plasticity around the grain boundary was attained. These results also suggest that the crack growth rate increased at locations where dislocation pile-ups impinge on the grain boundary. Adlakha and Solanki examined slip transmission across grain boundaries in α -Fe by MD calculation [152]. They found that hydrogen consistently increases the energy barrier for slip transmission, and claimed that the accumulation of plasticity induced by slip transmission provides an effective transport medium for hydrogen to be deposited at the GB. If the dislocations interacting with the GB are transporting hydrogen, the accumulation of H on GB can be enhanced, as incoming dislocations deposit hydrogen, emitted dislocations may remove hydrogen, but incoming-to-emitted dislocations rarely occur in a 1-to-1 ratio [153,154]. Additionally, the transfer of dislocation slip and the hydrogen-induced change in dislocation structure in the vicinity of a GB could increase the local disorder of the grain boundary allowing the boundary to accommodate more hydrogen

as additional low energy sites are generated.

Full intergranular fracture of Fe was achieved by cathodic charging of hydrogen at a current density of 20 A/m^2 [144], which is equivalent to a hydrogen gas pressure of 10^4 atm . At this pressure, the reduction of cohesive energy calculated by Wang et al. is around 37%. As mentioned in Section 3, recent studies of the microstructure beneath hydrogen-induced intergranular fracture surfaces [55,56] indicate that hydrogen-enhanced plasticity and the impact of that change on dislocation-GB interactions probably play a critical and determining role in establishing the conditions for intergranular fracture by boundary decohesion. Combining the experimental observations of high dislocation activity and these calculations, a mechanism for attaining high levels of hydrogen on grain boundaries becomes evident. Under this scenario, the final fracture behavior is not solely induced by the reduction of the grain boundary cohesive energy, but by a combined effect of hydrogen-enhanced plasticity and boundary decohesion.

7. Continuum modeling supporting the HELP mechanism

One of the main challenges in hydrogen embrittlement research is to establish a relationship between the hydrogen/deformation interactions observed at the microscopic scale and a fracture process that leads to macroscopic failure. Numerous studies have shown that hydrogen can increase the velocity of dislocations in various materials with different crystal structures [7,18–26]. In order to explain the effect of hydrogen on dislocation mobility, Birnbaum and Sofronis [13,14] investigated the interaction of a dislocation with another defect, such as another dislocation or an impurity atom, in the presence of hydrogen. Through their analytical and numerical analysis, they showed that, as the defects start to interact, the solute hydrogen atmosphere around the defects minimizes the total energy of the system, and thereby shields the elastic interaction between them. By weakening the barrier to dislocation motion, hydrogen accelerates dislocation mobility in the material. By elucidating a physically based explanation of elastic shielding, they established a scientific basis for the HELP mechanism as a viable explanation for hydrogen effects in metals.

By modeling the hydrogen distribution around an edge dislocation through discrete dilatation centers, Chateau et al. [123] numerically solved the coupled elasticity-diffusion problem, and

proposed an explanation for the increase in planarity observed in nickel single crystals due to the presence of hydrogen. They showed that hydrogen can increase the dissociation distance between the partial dislocations due to a decrease in the attractive force between their edge components. Such an increase in separation distance between the partials due to the shielding effect can have a large impact on the recombination work of partials (a 25% increase in equilibrium distance results in an increase of 60% of the recombination work); thus, the probability of cross-slip is decreased in the presence of hydrogen even if the stacking fault energy is unaffected by hydrogen. This influence on the separation of partials was also observed in a nickel-hydrogen system using the Monte Carlo calculation in [119].

Chateau et al. [155] also used discrete dislocation theory to study dislocation pile-ups against an obstacle at a crack tip in the presence of hydrogen. Hydrogen, by shielding the interactions between dislocations, caused the equilibrium positions of the dislocations in the pile-up to move toward the obstacle. Considering the same number of dislocations in the pile-up in the absence and presence of hydrogen, it was found that, despite the shift in dislocation position, the presence of hydrogen does not change the force acting on the obstacle in the plane of pile-up. However, out of this plane, hydrogen can increase the normal stress and facilitate the crack nucleation on other planes. This provides a viable explanation for the observation of micro-fracture occurring along alternating slip planes in a stress corrosion cracking experiment of austenitic stainless steel.

To account for the hydrogen-induced acceleration of dislocations in a larger-scale continuum model, Sofronis et al. [156] introduced local flow stress reduction that varies with hydrogen concentration into a material constitutive model. The model was not an exhaustive description of the response of the material's microstructure to the presence of hydrogen, but an attempt to incorporate the effect of hydrogen on dislocation mobility. Using this hydrogen-induced softening model, Sofronis et al. [156] derived the condition for shear localization of uniaxial specimens loaded under plane strain conditions. Shear localization is a form of plastic instability where the deformation is localized into a narrow band of intense shear. It was shown that hydrogen-induced material softening and lattice dilatation at the microscale can trigger macroscopic shear localization. It should be noted that such behavior is not possible for a hardening material under uniaxial tension in the absence of hydrogen.

Liang et al. [157] used a similar hydrogen-induced softening material model to ascertain the role of hydrogen in determining the onset of bifurcation of a homogenously deformed specimen under plane strain tension into necking or shear localization. The bifurcation was found by introducing either a geometric imperfection in the shape of uniaxial specimen or a local perturbation in the initial hydrogen concentration field. It was concluded that hydrogen can intensify and accelerate the deformation mode occurring in the absence of hydrogen, and can lead to earlier formation of localized shear bands. The results of these simulations showed that hydrogen can lower the threshold for plastic instability of materials, as has been observed experimentally [158].

The effect of hydrogen on void growth and coalescence was studied by Liang et al. [159] and Ahn et al. [160] utilizing hydrogen-induced local flow stress reduction within a unit cell analysis. In the unit cell approach, introduced by Koplik and Needleman [161] and Pardoen and Hutchinson [162] for non-hydrogen applications, the growth of a spherical void at the center of an axisymmetric cylindrical unit cell is analyzed through the finite element method. The unit cell is loaded macroscopically by principal axisymmetric stresses while triaxiality is held constant. Application of the model showed that, at high triaxialities in niobium [159], hydrogen accelerated the void growth with a negligible effect on void coalescence. On the other hand, at low triaxialities, hydrogen had a small effect on void growth but promoted void coalescence. For the case of A533B steel, Ahn et al. [160] demonstrated that hydrogen can promote void growth and coalescence at all levels of stress triaxialities with hydrogen having a decreasing effect on void coalescence as triaxiality is increased. The variation between the models of niobium and steel was attributed to the difference in trap density and strength of these systems. Ahn et al. [160] also observed that hydrogen caused the formation of a localized shear band emanating from the void surface in A533B steel at triaxiality equal to 1.

Ahn et al. [163] investigated the relationship between crack propagation and HELP using a two-scale microscopic/macrosopic modeling approach. Macroscopic crack propagation simulations were conducted using cohesive elements whose traction-separation laws were obtained through microscopic unit cell calculations. For the microscopic model, using the approach in [159] and [160], Ahn et al. [163] determined the response of individual void cells under different triaxialities with various hydrogen concentrations. Therefore, for each triaxiality and hydrogen concentration set, they constructed a traction-separation law for the unit cell. The

hydrogen-informed traction-separation laws were used in the cohesive elements laid ahead of a crack to study the crack propagation in A533B pressure vessel steel. Their simulations showed that hydrogen can greatly reduce the fracture initiation toughness and the tearing resistance (the R-curve slope) of the material, as is observed in experiments. They also showed that, by reducing the work of separation for materials around the voids ahead of the crack tip, hydrogen changes the mode of crack propagation.

Somerd़ay et al. [93] studied the effect of hydrogen on shear localization between microcracks. Their experimental study of hydrogen-assisted crack propagation in welds of nitrogen-strengthened austenitic stainless steel 21Cr-6Ni-9Mn (21-6-9) suggested that, as the main crack opens, parallel microcracks forms at various locations ahead of the crack. Upon further load increases, the ligaments between microcracks undergo an intense shear deformation and eventually fail, leading to linkage of the microcracks. Intense shear deformation was observed in the material adjacent to steps on the fracture surface. Using the hydrogen-induced softening model of [156], Somerd़ay et al. performed finite element analysis of parallel microcracks under uniaxial straining to evaluate the deformation ahead of a main crack. The results showed that while the ligament between the microcracks always experienced plastic deformation, hydrogen facilitated macroscopic intense shear deformation in the ligament. In the absence of hydrogen, plasticity was evenly spread throughout the ligament, but, in the presence of hydrogen, a localized band was formed between the microcracks.

Taking a synergistic action of HELP and hydrogen-enhanced decohesion (HEDE) into consideration, Novak et al. [164] presented a quantitative model for the prediction of brittle intergranular fracture of a high-strength martensitic steel in the presence of hydrogen. Hydrogen's role was assumed to be twofold: i) shielding the stress between dislocations and therefore increasing the number of dislocations in the pile-ups and ii) reducing the reversible work of interface separation. It was postulated that intergranular fracture in the presence of hydrogen is initiated by carbide/matrix interface decohesion due to impingement of dislocation pile-ups onto the carbides on the grain boundaries. Weakest link statistics was used to model the strength of the carbide/matrix interfaces. The interface strength was assumed to be related to the work of separation through the Smith model [165] which accounts for the dislocation pile-ups. Therefore, by reducing the work of separation, hydrogen reduces the carbide/matrix interface strength and promotes fracture triggered at the carbide/matrix interface. Novak et al. [164]

implemented the model in a finite element framework for single-edged notched bending specimens of AISI 4340 steel. The predicted fracture initiation bending loads for specimens charged with varying hydrogen concentrations were in a good agreement with experimental results.

In a follow up study, Nagao et al. [166] used the micromechanical model of Novak et al. [164] to model the hydrogen-influenced fracture response of the lath martensitic steels discussed in Section 4 [76,167]. By simulating fracture through a hydrogen-enhanced plasticity decohesion process, Nagao et al. found that the introduction of nanosized (Ti,Mo)C precipitates increases the resistance of these steels by reducing the amount of hydrogen at the high angle boundaries that would otherwise help advance intergranular or quasi-cleavage fracture.

In summary, continuum calculation approaches were used to explain and link the observed phenomena at the micro- and macro-scales. Hydrogen's effect on dislocation motion was explained through elastic shielding of the interaction of dislocations with other stress centers and increased slip planarity by increasing the recombination work of partial dislocations. By incorporating the effect of hydrogen on dislocation mobility in a continuum sense through local flow stress reduction in materials, accelerated localized shear band formation and void growth and coalescence promotion were demonstrated in the presence of hydrogen. Finally, the HELP mechanism was used to explain hydrogen-induced crack initiation and propagation resistance reduction.

8. Conclusions

While there are multiple proposed mechanisms for hydrogen-assisted failure, this review, by enumerating the experimental and numerical investigations underlying the hydrogen-enhanced localized plasticity (HELP) model, advances the thesis that HELP is the mechanism which best captures the fine nuances of the fracture behavior. There is clear evidence that hydrogen influences the behavior of dislocations, and this is exacerbated in regions of high hydrogen concentration. Due to the transportation of hydrogen by dislocations, this could produce a feedback loop of hydrogen-influenced dislocation behavior, which is evidenced by the dislocation structures observed directly underneath fracture features produced in hydrogen. It is

these recent results of the University of Illinois and the University of Wisconsin group that have finally brought strong evidence of how local hydrogen-enhanced plasticity can lead to enhanced failure: the mechanism of ***dislocation-mediated decohesion*** whereby the deformation structures formed due to the hydrogen-influence on dislocation motion are critical in establishing the conditions for failure. A process such as decohesion, especially of interfaces, may be the final failure mechanism, but atomistic simulations suggest that these processes are usually insufficient on their own and that it is the action of HELP, by helping accumulate sufficient hydrogen to influence the cohesion and by changing the local stress state, which is crucial to the embrittlement process.

There is a universal quality to the HELP mechanism, at least in structural materials such as nickel and ferritic, martensitic, and austenitic steels. Through recent studies, it has become clear that fractographic studies focused solely on fracture surface features are insufficient to determine failure processes. In fact, the main conclusion that could probably be drawn from fractography is that a complicated fracture surface indicates a complicated underlying microstructure. And without understanding that microstructure, there can be no understanding of the fracture process.

Even today, there still remains work to be done in the field of hydrogen embrittlement. The HELP mechanism still has its shortcomings, partly due to the lack of critical pieces of information. One of the most notable missing puzzle pieces is the exact location of hydrogen within the material, which new techniques such as atom probe tomography are showing promise of answering. Another critical question is at what point do other phenomenon, such as reduction of the cohesive energy of local features such as secondary phase boundaries, become the driving forces for failure. Atomistic simulations may also help answer some of these questions; however, their current greatest defects lie in the difficulty of modeling non-pristine crystals and encompassing conditions outside of absolute zero temperature and incredibly fast deformation rates, which correspond to conditions where hydrogen embrittlement is known to not occur.

Lastly, possibly the most crucial shortcoming of the hydrogen embrittlement field is a dearth of predictive models. Without predictive modeling, alloy design for hydrogen service still requires a great deal of testing, and relies upon old rules-of-thumb which, unfortunately, occasionally lead to catastrophic failures when subjected to regimes of more aggressive hydrogen embrittlement. Modeling is progressing, especially since continuum modeling can

help explain processes, but the critical point is the complexity of the phenomenon. Some of the work presented here has shown that using very complex continuum models, predictive capabilities are possible, since these complex models reflect the underlying physics of the problem. And that is the goal of future work: to physically capture enough features of the complex phenomenon that is hydrogen embrittlement so that proper materials selection and design can ensure safe operation in hydrogen environments. As visions of a hydrogen-based energy economy come further to the foreground, it becomes clear that a structured, physically based model of hydrogen embrittlement is needed to support this vision, and the HELP mechanism promises a clear scientific basis on which to build it.

Acknowledgements

The authors gratefully acknowledge the support of the International Institute for Carbon Neutral Energy Research (WPI-I2CNER), sponsored by the World Premier International Research Center Initiative (WPI), MEXT, Japan. The authors also acknowledge Prof. I.M. Robertson at the University of Wisconsin-Madison, and Dr. B.P. Somerday at the Southwest Research Institute for fruitful discussions.

References

- [1] Somerday, B. P., and Sofronis, P., eds., 2017, *Materials Performance in Hydrogen Environments: Proceedings of the 2016 International Hydrogen Conference*, ASME Press, New York, NY.
- [2] Johnson, W. H., 1875, “On Some Remarkable Changes Produced in Iron and Steel by the Action of Hydrogen and Acids,” Proc. R. Soc. London, **23**, pp. 168–179.
- [3] Robertson, I. M., Fenske, J., Martin, M. L., Bricena, M., Dadfarnia, M., Novak, P., Ahn, D. C., Sofronis, P., Liu, J. B., and Johnson, D. D., 2009, “Understanding How Hydrogen Influences the Mechanical Properties of Iron and Steel,” *Proceedings of the 2nd International Symposium on Steel Science (ISSS 2009)*, K. Higashida, and N. Tsuji, eds., The Iron and Steel Institute of Japan, Kyoto, Japan, pp. 63–72.
- [4] Nagao, A., Dadfarnia, M., Robertson, I. M., and Sofronis, P., 2016, “Hydrogen Embrittlement: Mechanisms,” *Encyclopedia of Iron, Steel, and Their Alloys*, R. Colas, and G.E. Totten, eds., Taylor and Francis, New York, NY, pp. 1768–1784.
- [5] Beachem, C. D., 1972, “A New Model for Hydrogen-Assisted Cracking (Hydrogen ‘Embrittlement’),” Metall. Trans., **3**(2), pp. 437–451.
- [6] Robertson, I. M., and Birnbaum, H. K., 1986, “An HVEM Study of Hydrogen Effects on

- the Deformation and Fracture of Nickel," *Acta Metall.*, **34**(3), pp. 353–366.
- [7] Bond, G. M., Robertson, I. M., and Birnbaum, H. K., 1987, "The Influence of Hydrogen on Deformation and Fracture Processes in High-Strength Aluminum Alloys," *Acta Metall.*, **35**(9), pp. 2289–2296.
- [8] Robertson, I. M., Tabata, T., Wei, W., Heubaum, F., and Birnbaum, H. K., 1984, "Hydrogen Embrittlement and Grain Boundary Fracture," *Scr. Metall.*, **18**(8), pp. 841–846.
- [9] Ferreira, P. J., Robertson, I. M., and Birnbaum, H. K., 1998, "Hydrogen Effects on the Interaction between Dislocations," *Acta Mater.*, **46**(5), pp. 1749–1757.
- [10] Ferreira, P. J., Robertson, I. M., and Birnbaum, H. K., 1999, "Hydrogen Effects on the Character of Dislocations in High-Purity Aluminum," *Acta Mater.*, **47**(10), pp. 2991–2998.
- [11] Myers, S. M., Baskes, M. I., Birnbaum, H. K., Corbett, J. W., DeLeo, G. G., Streicher, S. K., Haller, E. E., Jena, P., Johnson, N. M., Kirchheim, R., Pearton, S. J., and Stavola, M. J., 1992, "Hydrogen Interactions with Defects in Crystalline Solids," *Rev. Mod. Phys.*, **64**(2), pp. 559–617.
- [12] Matsumoto, R., Taketomi, S., Matsumoto, S., and Miyazaki, N., 2009, "Atomistic Simulations of Hydrogen Embrittlement," *Int. J. Hydrogen Energy*, **34**(23), pp. 9576–9584.
- [13] Birnbaum, H. K., and Sofronis, P., 1994, "Hydrogen-Enhanced Localized Plasticity—a Mechanism for Hydrogen-Related Fracture," *Mater. Sci. Eng. A*, **176**(1–2), pp. 191–202.
- [14] Sofronis, P., and Birnbaum, H. K., 1995, "Mechanics of the Hydrogen-Dislocation-Impurity Interactions—I. Increasing Shear Modulus," *J. Mech. Phys. Solids*, **43**(1), pp. 49–90.
- [15] Kimura, A., and Birnbaum, H. K., 1990, "Anomalous Strain Rate Dependence of the Serrated Flow in Ni-H and Ni-C-H Alloys," *Acta Metall. Mater.*, **38**(7), pp. 1343–1348.
- [16] Blakemore, J. S., 1970, "The Portevin-Le Chatelier Effect in Hydrogenated Nickel Alloys," *Metall. Trans.*, **1**(1), pp. 145–149.
- [17] Birnbaum, H. K., Robertson, I. M., Sofronis, P., and Teter, D. F., 1997, "Mechanisms of Hydrogen Related Fracture—a Review," *Corrosion-Deformation Interactions, CDI'96*, T. Magnin, ed., The Institute of Materials, London, pp. 172–195.
- [18] Tabata, T., and Birnbaum, H. K., 1983, "Direct Observations of the Effect of Hydrogen on the Behavior of Dislocations in Iron," *Scr. Metall.*, **17**(7), pp. 947–950.
- [19] Robertson, I. M., 2001, "The Effect of Hydrogen on Dislocation Dynamics," *Eng. Fract. Mech.*, **68**(6), pp. 671–692.
- [20] Sofronis, P., and Robertson, I. M., 2002, "Transmission Electron Microscopy Observations and Micromechanical/Continuum Models for the Effect of Hydrogen on the Mechanical Behaviour of Metals," *Philos. Mag. A*, **82**(17–18), pp. 3405–3413.
- [21] Sirois, E., and Birnbaum, H. K., 1992, "Effects of Hydrogen and Carbon on Thermally Activated Deformation in Nickel," *Acta Metall. Mater.*, **40**(6), pp. 1377–1385.
- [22] Wang, S., Hashimoto, N., and Ohnuki, S., 2013, "Effects of Hydrogen on Activation Volume and Density of Mobile Dislocations in Iron-Based Alloy," *Mater. Sci. Eng. A*, **562**, pp. 101–108.

- [23] Matsui, H., Kimura, H., and Moriya, S., 1979, "The Effect of Hydrogen on the Mechanical Properties of High Purity Iron I. Softening and Hardening of High Purity Iron by Hydrogen Charging during Tensile Deformation," *Mater. Sci. Eng.*, **40**(2), pp. 207–216.
- [24] Moriya, S., Matsui, H., and Kimura, H., 1979, "The Effect of Hydrogen on the Mechanical Properties of High Purity Iron II. Effect of Quenched-in Hydrogen below Room Temperature," *Mater. Sci. Eng.*, **40**(2), pp. 217–225.
- [25] Matsui, H., Kimura, H., and Kimura, A., 1979, "The Effect of Hydrogen on the Mechanical Properties of High Purity Iron III. The Dependence of Softening on Specimen Size and Charging Current Density," *Mater. Sci. Eng.*, **40**(2), pp. 227–234.
- [26] Abraham, D. P., and Altstetter, C. J., 1995, "Hydrogen-Enhanced Localization of Plasticity in an Austenitic Stainless Steel," *Metall. Mater. Trans. A*, **26**(11), pp. 2859–2871.
- [27] Eastman, J., Heubaum, F., Matsumoto, T., and Birnbaum, H. K., 1982, "The Effect of Hydrogen on the Solid Solution Strengthening and Softening of Nickel," *Acta Metall.*, **30**(8), pp. 1579–1586.
- [28] Louthan Jr., M. R., Caskey Jr., G. R., Donovan, J. A., and Rawl, D. E., 1972, "Hydrogen Embrittlement of Metals," *Mater. Sci. Eng.*, **10**(6), pp. 357–368.
- [29] Itoh, G., Jinkoji, T., Kanno, M., and Koyama, K., 1997, "Effect of Impurity Hydrogen on the Deformation and Fracture in an Al-5 Mass Pct Mg Alloy," *Metall. Mater. Trans. A*, **28**(11), pp. 2291–2295.
- [30] Shih, D. S., Robertson, I. M., and Birnbaum, H. K., 1988, "Hydrogen Embrittlement of α Titanium: In Situ TEM Studies," *Acta Metall.*, **36**(1), pp. 111–124.
- [31] Sofronis, P., 1995, "The Influence of Mobility of Dissolved Hydrogen on the Elastic Response of a Metal," *J. Mech. Phys. Solids*, **43**(9), pp. 1385–1407.
- [32] Ferreira, P. J., Robertson, I. M., and Birnbaum, H. K., 1996, "The Influence of Hydrogen on the Stacking Fault Energy of an Austenitic Stainless Steel," *Mater. Sci. Forum*, **207–209**, pp. 93–96.
- [33] Chen, Y. Z., Barth, H. P., Deutges, M., Borchers, C., Liu, F., and Kirchheim, R., 2013, "Increase in Dislocation Density in Cold-Deformed Pd Using H as a Temporary Alloying Addition," *Scr. Mater.*, **68**(9), pp. 743–746.
- [34] Kirchheim, R., 2010, "Revisiting Hydrogen Embrittlement Models and Hydrogen-Induced Homogeneous Nucleation of Dislocations," *Scr. Mater.*, **62**(2), pp. 67–70.
- [35] Kirchheim, R., 2007, "Reducing Grain Boundary, Dislocation Line and Vacancy Formation Energies by Solute Segregation. I. Theoretical Background," *Acta Mater.*, **55**(15), pp. 5129–5138.
- [36] Kirchheim, R., 2007, "Reducing Grain Boundary, Dislocation Line and Vacancy Formation Energies by Solute Segregation II. Experimental Evidence and Consequences," *Acta Mater.*, **55**(15), pp. 5139–5148.
- [37] Lu, G., Zhang, Q., Kioussis, N., and Kaxiras, E., 2001, "Hydrogen-Enhanced Local Plasticity in Aluminum: An Ab Initio Study," *Phys. Rev. Lett.*, **87**(9), p. 095501:1-4.
- [38] Wen, M., Fukuyama, S., and Yokogawa, K., 2003, "Atomistic Simulations of Effect of

- Hydrogen on Kink-Pair Energetics of Screw Dislocations in Bcc Iron," *Acta Mater.*, **51**(6), pp. 1767–1773.
- [39] Wen, M., Zhang, L., An, B., Fukuyama, S., and Yokogawa, K., 2009, "Hydrogen-Enhanced Dislocation Activity and Vacancy Formation during Nanoindentation of Nickel," *Phys. Rev. B*, **80**(9), p. 094113:1-5.
 - [40] Maier, H. J., and Kaesche, H., 1990, "Environmental Effects on the Dislocation Arrangement of Fatigued Low Alloy Steel," *Scr. Metall. Mater.*, **24**(1), pp. 123–128.
 - [41] Moreno-Gobbi, A., Zamir, G., and Eiras, J. A., 2011, "Ultrasonic Investigation of the Interaction of Hydrogen-Dislocations in Copper Crystals," *Mater. Sci. Eng. A*, **528**(12), pp. 4255–4258.
 - [42] San Juan, J., Fantozzi, G., No, M. L., and Esnouf, C., 1987, "Hydrogen Snoek-Koster Relaxation in Iron," *J. Phys. F Met. Phys.*, **17**(4), pp. 837–848.
 - [43] Robertson, I. M., Birnbaum, H. K., and Sofronis, P., 2009, "Hydrogen Effects on Plasticity," *Dislocations in Solids*, J.P. Hirth, and L. Kubin, eds., Springer Netherlands, Dordrecht, pp. 367–381.
 - [44] Deutges, M., Barth, H. P., Chen, Y., Borchers, C., and Kirchheim, R., 2015, "Hydrogen Diffusivities as a Measure of Relative Dislocation Densities in Palladium and Increase of the Density by Plastic Deformation in the Presence of Dissolved Hydrogen," *Acta Mater.*, **82**, pp. 266–274.
 - [45] Wang, S., Nagao, A., Edalati, K., Horita, Z., and Robertson, I. M., 2017, "Influence of Hydrogen on Dislocation Self-Organization in Ni," *Acta Mater.*, **135**, pp. 96–102.
 - [46] Deutges, M., Knorr, I., Borchers, C., Volkert, C. A., and Kirchheim, R., 2013, "Influence of Hydrogen on the Deformation Morphology of Vanadium (100) Micropillars in the α -Phase of the Vanadium-hydrogen System," *Scr. Mater.*, **68**(1), pp. 71–74.
 - [47] Delafosse, D., 2012, "Hydrogen Effects on the Plasticity of Fcc Crystals," *Gaseous Hydrogen Embrittlement of Materials in Energy Technologies*, R.P. Gangloff, and B.P. Somerday, eds., Woodhead Publishing, Cambridge, UK, pp. 247–285.
 - [48] Martin, M. L., Nagao, A., Robertson, I. M., and Sofronis, P., 2014, "Hydrogen-Enhanced Plasticity and Failure Revisited," *2012 International Hydrogen Conference: Hydrogen-Materials Interactions*, B.P. Somerday, and P. Sofronis, eds., ASME Press, New York, NY, pp. 489–496.
 - [49] Smith, R. L., Moore, G. A., and Brick, R. M., 1952, "Mechanical Properties of High-Purity Iron-Carbon Alloy at Low Temperature," *Mechanical Properties of Metals at Low Temperatures*, National Bureau of Standards, pp. 153–179.
 - [50] Martin, M. L., Robertson, I. M., and Sofronis, P., 2011, "Interpreting Hydrogen-Induced Fracture Surfaces in Terms of Deformation Processes: A New Approach," *Acta Mater.*, **59**(9), pp. 3680–3687.
 - [51] Lassila, D. H., and Birnbaum, H. K., 1986, "The Effect of Diffusive Hydrogen Segregation on Fracture of Polycrystalline Nickel," *Acta Metall.*, **34**(7), pp. 1237–1243.
 - [52] Lassila, D. H., and Birnbaum, H. K., 1987, "Intergranular Fracture of Nickel: The Effect of

- Hydrogen-Sulphur Co-Segregation," *Acta Metall.*, **35**(7), pp. 1815–1822.
- [53] Hugo, R. C., and Hoagland, R. G., 1998, "In-Situ TEM Observation of Aluminum Embrittlement by Liquid Gallium," *Scr. Mater.*, **38**(3), pp. 523–529.
- [54] Oriani, R. A., and Josephic, P. H., 1974, "Equilibrium Aspects of Hydrogen-Induced Cracking of Steels," *Acta Metall.*, **22**(9), pp. 1065–1074.
- [55] Martin, M. L., Somerday, B. P., Ritchie, R. O., Sofronis, P., and Robertson, I. M., 2012, "Hydrogen-Induced Intergranular Failure in Nickel Revisited," *Acta Mater.*, **60**(6–7), pp. 2739–2745.
- [56] Wang, S., Martin, M. L., Sofronis, P., Ohnuki, S., Hashimoto, N., and Robertson, I. M., 2014, "Hydrogen-Induced Intergranular Failure of Iron," *Acta Mater.*, **69**, pp. 275–282.
- [57] Martin, M. L., 2012, "A New Approach to Discovering the Fundamental Mechanisms of Hydrogen Failure," PhD Dissertation, University of Illinois at Urbana-Champaign.
- [58] Keller, C., Hug, E., and Feaugas, X., 2011, "Microstructural Size Effects on Mechanical Properties of High Purity Nickel," *Int. J. Plast.*, **27**(4), pp. 635–654.
- [59] Murakami, Y., Kanezaki, T., and Mine, Y., 2010, "Hydrogen Effect against Hydrogen Embrittlement," *Metall. Mater. Trans. A*, **41**(10), pp. 2548–2562.
- [60] Martin, M. L., Sofronis, P., Robertson, I. M., Awane, T., and Murakami, Y., 2013, "A Microstructural Based Understanding of Hydrogen-Enhanced Fatigue of Stainless Steels," *Int. J. Fatigue*, **57**, pp. 28–36.
- [61] Ro, Y. J., Agnew, S. R., and Gangloff, R. P., 2012, "Effect of Environment on Fatigue Crack Wake Dislocation Structure in Al-Cu-Mg," *Metall. Mater. Trans. A*, **43**(7), pp. 2275–2292.
- [62] Efron, A., Lifshitz, Y., Lewkowicz, I., and Mintz, M. H., 1989, "The Kinetics and Mechanism of Titanium Hydride Formation," *J. Less-Common Met.*, **153**(1), pp. 23–34.
- [63] Lovelace, B., Bakhru, H., Haberl, A. W., and Benenson, R. E., 2007, "Microbeam Analysis of Hydrogen near a Crack Tip in Titanium," *Nucl. Instruments Methods Phys. Res. Sect. B*, **261**(1–2), pp. 477–482.
- [64] Dadfarnia, M., Martin, M. L., Nagao, A., Sofronis, P., and Robertson, I. M., 2015, "Modeling Hydrogen Transport by Dislocations," *J. Mech. Phys. Solids*, **78**, pp. 511–525.
- [65] Garrison Jr., W. M., and Moody, N. R., 2012, "Hydrogen Embrittlement of High Strength Steels," *Gaseous Hydrogen Embrittlement of Materials in Energy Technologies*, R.P. Gangloff, and B.P. Somerday, eds., Woodhead Publishing, Cambridge, UK, pp. 421–492.
- [66] Turnbull, A., and Zhou, S., 2014, "Environment Assisted Cracking of Steam Turbine Blade Steels - a Consistent Rationalization Based on Hydrogen Assisted Cracking," *Hydrogen-Materials Interactions: Proceedings of the 2012 International Hydrogen Conference*, B.P. Somerday, and P. Sofronis, eds., ASME Press, New York, NY, pp. 91–100.
- [67] Nagumo, M., 2016, *Fundamentals of Hydrogen Embrittlement*, Springer, New York, NY.
- [68] Kimura, Y., Inoue, T., Akiyama, E., and Tsuzaki, K., 2014, "Hydrogen Embrittlement in Ultrafine Elongated Grain Structure Steel Processed by Warm Tempforming," *Hydrogen-Materials Interactions: Proceedings of the 2012 International Hydrogen Conference*, B.P.

- Somerday, and P. Sofronis, eds., ASME Press, New York, NY, pp. 101–110.
- [69] Shibata, A., Murata, T., and Tsuji, N., 2014, “Crystallographic Analysis of Hydrogen-Related Fracture in Medium Carbon Martensitic Steel,” *Hydrogen-Materials Interactions: Proceedings of the 2012 International Hydrogen Conference*, B.P. Somerday, and P. Sofronis, eds., ASME Press, New York, NY, pp. 111–118.
- [70] Matsuoka, T., Shibata, A., and Tsuji, N., 2014, “Effect of Microstructure of Martensite on Hydrogen Embrittlement in 8Ni-0.1C Steel,” *Hydrogen-Materials Interactions: Proceedings of the 2012 International Hydrogen Conference*, B.P. Somerday, and P. Sofronis, eds., ASME Press, New York, NY, pp. 119–126.
- [71] Nagao, A., Eftink, B. P., Dadfarnia, M., Somerday, B. P., and Sofronis, P., 2014, “The Effect of Nano-Sized TiC Precipitates on Hydrogen Embrittlement of Tempered Lath Martensitic Steel,” *Hydrogen-Materials Interactions: Proceedings of the 2012 International Hydrogen Conference*, B.P. Somerday, and P. Sofronis, eds., ASME Press, New York, NY, pp. 127–135.
- [72] Rehrl, J., Mraczek, K., Pichler, A., and Werner, E., 2014, “Influence of Microstructure and Ti(C,N) on the Susceptibility to Hydrogen Embrittlement of AHSS Grades for the Automotive Industry,” *Hydrogen-Materials Interactions: Proceedings of the 2012 International Hydrogen Conference*, B.P. Somerday, and P. Sofronis, eds., ASME Press, New York, NY, pp. 137–146.
- [73] Doshida, T., Suzuki, H., Takai, K., Oshima, N., and Hirade, T., 2012, “Enhanced Lattice Defect Formation Associated with Hydrogen and Hydrogen Embrittlement under Elastic Stress of a Tempered Martensitic Steel,” *ISIJ Int.*, **52**(2), pp. 198–207.
- [74] Shibata, A., Takahashi, H., and Tsuji, N., 2012, “Microstructural and Crystallographic Features of Hydrogen-Related Crack Propagation in Low Carbon Martensitic Steel,” *ISIJ Int.*, **52**(2), pp. 208–212.
- [75] Nagao, A., Hayashi, K., Oi, K., and Mitao, S., 2012, “Effect of Uniform Distribution of Fine Cementite on Hydrogen Embrittlement of Low Carbon Martensitic Steel Plates,” *ISIJ Int.*, **52**(2), pp. 213–221.
- [76] Nagao, A., Smith, C. D., Dadfarnia, M., Sofronis, P., and Robertson, I. M., 2012, “The Role of Hydrogen in Hydrogen Embrittlement Fracture of Lath Martensitic Steel,” *Acta Mater.*, **60**(13–14), pp. 5182–5189.
- [77] Beachem, C. D., 1973, “Orientation of Cleavage Facets in Tempered Martensite (Quasi-Cleavage) by Single Surface Trace Analysis,” *Metall. Trans.*, **4**(8), pp. 1999–2000.
- [78] Kim, Y. H., and Morris, J. W., 1983, “The Nature of Quasicleavage Fracture in Tempered 5.5Ni Steel after Hydrogen Charging,” *Metall. Trans. A*, **14**(9), pp. 1883–1888.
- [79] Shibata, A., Murata, T., Takahashi, H., Matsuoka, T., and Tsuji, N., 2015, “Characterization of Hydrogen-Related Fracture Behavior in as-Quenched Low-Carbon Martensitic Steel and Tempered Medium-Carbon Martensitic,” *Metall. Mater. Trans. A*, **46**(12), pp. 5685–5696.
- [80] Pioszak, G. L., and Gangloff, R. P., 2017, “Hydrogen Environment Assisted Cracking of Modern Ultra-High Strength Martensitic Steels,” *Metall. Mater. Trans. A*, **48**(9), pp. 4025–

4045.

- [81] Shibata, A., Matsuoka, T., Ueno, A., and Tsuji, N., 2017, "Fracture Surface Topography Analysis of the Hydrogen-Related Fracture Propagation Process in Martensitic Steel," *Int. J. Fract.*, **205**(1), pp. 73–82.
- [82] Nagao, A., Smith, C. D., Dadfarnia, M., Sofronis, P., and Robertson, I. M., 2014, "Interpretation of Hydrogen-Induced Fracture Surface Morphologies for Lath Martensitic Steel," *Procedia Mater. Sci.*, **3**, pp. 1700–1705.
- [83] Nagao, A., Kuramoto, S., Ichitani, K., and Kanno, M., 2001, "Visualization of Hydrogen Transport in High Strength Steels Affected by Stress Fields and Hydrogen Trapping," *Scr. Mater.*, **45**(10), pp. 1227–1232.
- [84] San Marchi, C., 2012, "Hydrogen Embrittlement of Stainless Steels and Their Welds," *Gaseous Hydrogen Embrittlement of Materials in Energy Technologies*, R.P. Gangloff, and B.P. Somerday, eds., Woodhead Publishing, Cambridge, UK, pp. 592–623.
- [85] Kanezaki, T., Narazaki, C., Mine, Y., Matsuoka, S., and Murakami, Y., 2008, "Effects of Hydrogen on Fatigue Crack Growth Behavior of Austenitic Stainless Steels," *Int. J. Hydrogen Energy*, **33**(10), pp. 2604–2619.
- [86] Omura, T., and Nakamura, J., 2012, "Hydrogen Embrittlement Properties of Stainless and Low Alloy Steels in High Pressure Gaseous Hydrogen Environment," *ISIJ Int.*, **52**(2), pp. 234–239.
- [87] Whiteman, M. B., and Troiano, A. R., 1965, "Hydrogen Embrittlement of Austenitic Stainless Steel," *Corrosion*, **21**(2), pp. 53–56.
- [88] Moody, N. R., Robinson, S. L., and Garrison Jr., W. M., 1990, "Hydrogen Effects on the Properties and Fracture Modes of Iron-Based Alloys," *Res Mech.*, **30**(2), pp. 143–206.
- [89] Eliezer, D., Chakrapani, D. G., Altstetter, C. J., and Pugh, E. N., 1979, "The Influence of Austenite Stability on the Hydrogen Embrittlement and Stress-Corrosion Cracking of Stainless Steel," *Metall. Trans. A*, **10**(7), pp. 935–941.
- [90] Ulmer, D. G., and Altstetter, C. J., 1991, "Hydrogen-Induced Strain Localization and Failure of Austenitic Stainless Steels at High Hydrogen Concentrations," *Acta Metall. Mater.*, **39**(6), pp. 1237–1248.
- [91] San Marchi, C., and Somerday, B. P., 2012, *Technical Reference for Hydrogen Compatibility of Materials, SAND2012-7321*, Sandia National Laboratories, Livermore, CA.
- [92] San Marchi, C., Somerday, B. P., Tang, X., and Schiroky, G. H., 2008, "Effects of Alloy Composition and Strain Hardening on Tensile Fracture of Hydrogen-Precharged Type 316 Stainless Steels," *Int. J. Hydrogen Energy*, **33**(2), pp. 889–904.
- [93] Somerday, B. P., Dadfarnia, M., Balch, D. K., Nibur, K. A., Cadden, C. H., and Sofronis, P., 2009, "Hydrogen-Assisted Crack Propagation in Austenitic Stainless Steel Fusion Welds," *Metall. Mater. Trans. A*, **40**(10), pp. 2350–2362.
- [94] Jackson, H. F., Nibur, K. A., San Marchi, C., Puskar, J. D., and Somerday, B. P., 2012, "Hydrogen-Assisted Crack Propagation in 304L/308L and 21Cr-6Ni-9Mn/308L Austenitic

- Stainless Steel Fusion Welds," Corros. Sci., **60**, pp. 136–144.
- [95] Allain, S., Chateau, J., Bouaziz, O., Migot, S., and Guelton, N., 2004, "Correlations between the Calculated Stacking Fault Energy and the Plasticity Mechanisms in Fe–Mn–C Alloys," Mater. Sci. Eng. A, **387–389**, pp. 158–162.
- [96] Rozenak, P., and Eliezer, D., 1987, "Phase Changes Related to Hydrogen-Induced Cracking in Austenitic Stainless Steel," Acta Metall., **35**(9), pp. 2329–2340.
- [97] Müllner, P., Solenthaler, C., Uggowitzer, P. J., and Speidel, M. O., 1994, "Brittle Fracture in Austenitic Steel," Acta Metall. Mater., **42**(7), pp. 2211–2217.
- [98] Jackson, H., San Marchi, C., Balch, D. K., Somerday, B. P., and Michael, J., 2016, "Effects of Low Temperature on Hydrogen-Assisted Crack Growth in Forged 304L Austenitic Stainless Steel," Metall. Mater. Trans. A, **47**(8), pp. 4334–4350.
- [99] Rozenak, P., Robertson, I. M., and Birnbaum, H. K., 1990, "HVEM Studies of the Effects of Hydrogen on the Deformation and Fracture of AISI Type 316 Austenitic Stainless Steel," Acta Metall. Mater., **38**(11), pp. 2031–2040.
- [100] Nibur, K. A., Bahr, D. F., and Somerday, B. P., 2006, "Hydrogen Effects on Dislocation Activity in Austenitic Stainless Steel," Acta Mater., **54**(10), pp. 2677–2684.
- [101] Michler, T., San Marchi, C., Naumann, J., Weber, S., and Martin, M., 2012, "Hydrogen Environment Embrittlement of Stable Austenitic Steels," Int. J. Hydrogen Energy, **37**(21), pp. 16231–16246.
- [102] Hatano, M., Fujinami, M., Arai, K., Fujii, H., and Nagumo, M., 2014, "Hydrogen Embrittlement of Austenitic Stainless Steels Revealed by Deformation Microstructures and Strain-Induced Creation of Vacancies," Acta Mater., **67**, pp. 342–353.
- [103] Koyama, M., Okazaki, S., Sawaguchi, T., and Tsuzaki, K., 2016, "Hydrogen Embrittlement Susceptibility of Fe-Mn Binary Alloys with High Mn Content: Effects of Stable and Metastable ϵ -Martensite, and Mn Concentration," Metall. Mater. Trans. A, **47**(6), pp. 2656–2673.
- [104] Han, G., He, J., Fukuyama, S., and Yokogawa, K., 1998, "Effect of Strain-Induced Martensite on Hydrogen Environment Embrittlement of Sensitized Austenitic Stainless Steels at Low Temperatures," Acta Mater., **46**(13), pp. 4559–4570.
- [105] Jackson, H. F., San Marchi, C., Balch, D. K., and Somerday, B. P., 2013, "Effect of Low Temperature on Hydrogen-Assisted Crack Propagation in 304L/308L Austenitic Stainless Steel Fusion Welds," Corros. Sci., **77**, pp. 210–221.
- [106] San Marchi, C., Nibur, K. A., Balch, D. K., Somerday, B. P., Tang, X., Schiroky, G. H., and Michler, T., 2009, "Hydrogen-Assisted Fracture of Austenitic Stainless Steels," *Effects of Hydrogen on Materials*, B.P. Somerday, P. Sofronis, and R.H. Jones, eds., ASM International, Metal Park, OH, pp. 88–96.
- [107] Nibur, K. A., Somerday, B. P., Balch, D. K., and San Marchi, C., 2009, "The Role of Localized Deformation in Hydrogen-Assisted Crack Propagation in 21Cr-6Ni-9Mn Stainless Steel," Acta Mater., **57**(13), pp. 3795–3809.
- [108] Koyama, M., Springer, H., Merzlikin, S. V., Tsuzaki, K., Akiyama, E., and Raabe, D., 2014,

- “Hydrogen Embrittlement Associated with Strain Localization in a Precipitation-Hardened Fe-Mn-Al-C Light Weight Austenitic Steel,” Int. J. Hydrogen Energy, **39**(9), pp. 4634–4646.
- [109] Koyama, M., Akiyama, E., Lee, Y. K., Raabe, D., and Tsuzaki, K., 2017, “Overview of Hydrogen Embrittlement in High-Mn Steels,” Int. J. Hydrogen Energy, **42**(17), pp. 12706–12723.
- [110] Watanabe, T., and Tsurekawa, S., 1999, “The Control of Brittleness and Development of Desirable Mechanical Properties in Polycrystalline Systems by Grain Boundary Engineering,” Acta Mater., **47**(15–16), pp. 4171–4185.
- [111] Bechtle, S., Kumar, M., Somerday, B. P., Launey, M. E., and Ritchie, R. O., 2009, “Grain-Boundary Engineering Markedly Reduces Susceptibility to Intergranular Hydrogen Embrittlement in Metallic Materials,” Acta Mater., **57**(14), pp. 4148–4157.
- [112] Koyama, M., Akiyama, E., Tsuzaki, K., and Raabe, D., 2013, “Hydrogen-Assisted Failure in a Twinning-Induced Plasticity Steel Studied under in Situ Hydrogen Charging by Electron Channeling Contrast Imaging,” Acta Mater., **61**(12), pp. 4607–4618.
- [113] Koyama, M., Akiyama, E., Sawaguchi, T., Ogawa, K., Kireeva, I. V., Chumlyakov, Y. I., and Tsuzaki, K., 2013, “Hydrogen-Assisted Quasi-Cleavage Fracture in a Single Crystalline Type 316 Austenitic Stainless Steel,” Corros. Sci., **75**, pp. 345–353.
- [114] An, B., Itouga, H., Iijima, T., San Marchi, C., and Somerday, B. P., 2013, “Hydrogen-Assisted Twin Boundary Fracture of Type 304 Austenitic Stainless Steel at Low Temperature Investigated by Scanning Probe Microscopy,” *Proceedings of the ASME 2013 Pressure Vessels and Piping Conference (PVP2013)*, ASME, July 14–18, 2013, Paris, France, pp. PVP2013-97355.
- [115] Taketomi, S., Matsumoto, R., and Miyazaki, N., 2008, “Atomistic Simulation of the Effects of Hydrogen on the Mobility of Edge Dislocation in Alpha Iron,” J. Mater. Sci., **43**(3), pp. 1166–1169.
- [116] Wang, S., Hashimoto, N., and Ohnuki, S., 2013, “Hydrogen-Induced Change in Core Structures of {110}{111} Edge and {110}{111} Screw Dislocations in Iron,” Sci. Rep., **3**, p. 2760:1–4.
- [117] Itakura, M., Kaburaki, H., Yamaguchi, M., and Okita, T., 2013, “The Effect of Hydrogen Atoms on the Screw Dislocation Mobility in Bcc Iron: A First-Principles Study,” Acta Mater., **61**(18), pp. 6857–6867.
- [118] Itakura, M., Kaburaki, H., and Yamaguchi, M., 2012, “First-Principles Study on the Mobility of Screw Dislocations in Bcc Iron,” Acta Mater., **60**(9), pp. 3698–3710.
- [119] von Pezold, J., Lymperakis, L., and Neugebauer, J., 2011, “Hydrogen-Enhanced Local Plasticity at Dilute Bulk H Concentrations: The Role of H-H Interactions and the Formation of Local Hydrides,” Acta Mater., **59**(8), pp. 2969–2980.
- [120] Wagih, M., Tang, Y., Hatem, T., and El-Awady, J. A., 2015, “Discerning Enhanced Dislocation Plasticity in Hydrogen-Charged α -Iron Nano-Crystals,” Mater. Res. Lett., **3**(4), pp. 184–189.
- [121] Ventelon, L., Willaime, F., Clouet, E., and Rodney, D., 2013, “Ab Initio Investigation of

- the Peierls Potential of Screw Dislocations in Bcc Fe and W," *Acta Mater.*, **61**(11), pp. 3973–3985.
- [122] Proville, L., Ventelon, L., and Rodney, D., 2013, "Prediction of the Kink-Pair Formation Enthalpy on Screw Dislocations in α -Iron by a Line Tension Model Parametrized on Empirical Potentials and First-Principles Calculations," *Phys. Rev. B*, **87**(14), p. 144106:1–8.
- [123] Chateau, J. P., Delafosse, D., and Magnin, T., 2002, "Numerical Simulations of Hydrogen-Dislocation Interactions in Fcc Stainless Steels. Part I: Hydrogen-Dislocation Interactions in Bulk Crystals," *Acta Mater.*, **50**(6), pp. 1507–1522.
- [124] Windle, A. H., and Smith, G. C., 1968, "The Effect of Hydrogen on the Plastic Deformation of Nickel Single Crystals," *Met. Sci. J.*, **2**, pp. 187–191.
- [125] Angelo, J. E., Moody, N. R., and Baskes, M. I., 1995, "Trapping of Hydrogen to Lattice Defects in Nickel," *Model. Simul. Mater. Sci. Eng.*, **3**(3), pp. 289–307.
- [126] Baskes, M. I., Sha, X., Angelo, J. E., and Moody, N. R., 1997, "Trapping of Hydrogen to Lattice Defects in Nickel," *Model. Simul. Mater. Sci. Eng.*, **5**(6), pp. 651–652.
- [127] Hirth, J. P., and Rice, J. R., 1980, "On the Thermodynamics of Adsorption at Interfaces as It Influences Decohesion," *Metall. Trans. A*, **11**(9), pp. 1501–1511.
- [128] Rice, J. R., and Wang, J.-S., 1989, "Embrittlement of Interfaces by Solute Segregation," *Mater. Sci. Eng. A*, **107**(1–2), pp. 23–40.
- [129] Wu, R., Freeman, A. J., and Olson, G. B., 1994, "First Principles Determination of the Effects of Phosphorus and Boron on Iron Grain Boundary Cohesion," *Science*, **265**(5170), pp. 376–80.
- [130] Wu, R., Freeman, A. J., and Olson, G. B., 1996, "Effects of Carbon on Fe-Grain-Boundary Cohesion: First-Principles Determination," *Phys. Rev. B*, **53**(11), pp. 7504–7509.
- [131] Zhong, L., Wu, R., Freeman, A. J., and Olson, G. B., 1997, "Effects of Mn Additions on the P Embrittlement of the Fe Grain Boundary," *Phys. Rev. B*, **55**(17), pp. 11133–11137.
- [132] Geng, W. T., Freeman, A. J., Wu, R., Geller, C. B., and Raynolds, J. E., 1999, "Embritting and Strengthening Effects of Hydrogen, Boron, and Phosphorus on a $\Sigma 5$ Nickel Grain Boundary," *Phys. Rev. B*, **60**(10), pp. 7149–7155.
- [133] Zhong, L., Wu, R., Freeman, A. J., and Olson, G. B., 2000, "Charge Transfer Mechanism of Hydrogen-Induced Intergranular Embrittlement of Iron," *Phys. Rev. B*, **62**(21), pp. 13938–13941.
- [134] Geng, W. T., Freeman, A. J., and Olson, G. B., 2001, "Influence of Alloying Additions on Grain Boundary Cohesion of Transition Metals: First-Principles Determination and Its Phenomenological Extension," *Phys. Rev. B*, **63**(16), p. 165415:1–9.
- [135] Geng, W. T., Freeman, A. J., Olson, G. B., Tateyama, Y., and Ohno, T., 2005, "Hydrogen-Promoted Grain Boundary Embrittlement and Vacancy Activity in Metals: Insights from Ab Initio Total Energy Calculations," *Mater. Trans.*, **46**(4), pp. 756–760.
- [136] Anderson, P. M., Wang, J., and Rice, J. R., 1990, "Thermodynamic and Mechanical Models of Interfacial Embrittlement," *Innovations in Ultrahigh-Strength Steel Technology*,

- G.B. Olson, M. Azrin, and E.S. Wright, eds., pp. 619–649.
- [137] Yamaguchi, M., Kameda, J., Ebihara, K., Itakura, M., and Kaburaki, H., 2012, “Mobile Effect of Hydrogen on Intergranular Decohesion of Iron : First-Principles Calculations,” *Philos. Mag.*, **92**(11), pp. 1349–1368.
- [138] Yamaguchi, M., Ebihara, K., Itakura, M., Kadoyoshi, T., Suzudo, T., and Kaburaki, H., 2011, “First-Principles Study on the Grain Boundary Embrittlement of Metals by Solute Segregation: Part II. Metal (Fe, Al, Cu)-Hydrogen (H) Systems,” *Metall. Mater. Trans. A*, **42**(2), pp. 330–339.
- [139] Kirchheim, R., Somerday, B. P., and Sofronis, P., 2015, “Chemomechanical Effects on the Separation of Interfaces Occurring during Fracture with Emphasis on the Hydrogen-Iron and Hydrogen-Nickel System,” *Acta Mater.*, **99**, pp. 87–98.
- [140] Solanki, K. N., Tschoop, M. A., Bhatia, M. A., and Rhodes, N. R., 2013, “Atomistic Investigation of the Role of Grain Boundary Structure on Hydrogen Segregation and Embrittlement in α -Fe,” *Metall. Mater. Trans. A*, **44**(3), pp. 1365–1375.
- [141] Yuasa, M., Nishihara, D., Mabuchi, M., and Chino, Y., 2012, “Hydrogen Embrittlement in a Magnesium Grain Boundary: A First-Principles Study,” *J. Phys. Condens. Matter*, **24**(8), p. 085701:1–9.
- [142] McMahon Jr., C. J., 2001, “Hydrogen-Induced Intergranular Fracture of Steels,” *Eng. Fract. Mech.*, **68**(6), pp. 773–788.
- [143] Shin, K. S., and Meshii, M., 1983, “Effect of Sulfur Segregation and Hydrogen Charging on Intergranular Fracture of Iron,” *Acta Metall.*, **31**(10), pp. 1559–1566.
- [144] Kimura, A., and Kimura, H., 1984, “Effect of Carbon on the Hydrogen Induced Grain Boundary Fracture in Iron,” *Trans. Japan Inst. Met.*, **25**(6), pp. 411–419.
- [145] Wang, S., Martin, M. L., Robertson, I. M., and Sofronis, P., 2016, “Effect of Hydrogen Environment on the Separation of Fe Grain Boundaries,” *Acta Mater.*, **107**, pp. 279–288.
- [146] Dadfarnia, M., Nagao, A., Wang, S., Martin, M. L., Somerday, B. P., and Sofronis, P., 2015, “Recent Advances on Hydrogen Embrittlement of Structural Materials,” *Int. J. Fract.*, **196**(1–2), pp. 223–243.
- [147] Stull, D. R., and Prophet, H., 1971, *JANAF Thermochemical Tables, NSRDS-NBS37 (2nd Edition)*, National Standard Reference Data System.
- [148] Rice, J. R., 1978, “Thermodynamics of the Quasi-Static Growth of Griffith Cracks,” *J. Mech. Phys. Solids*, **26**(2), pp. 61–78.
- [149] Taketomi, S., Matsumoto, R., and Miyazaki, N., 2010, “Atomistic Study of the Effect of Hydrogen on Dislocation Emission from a Mode II Crack Tip in Alpha Iron,” *Int. J. Mech. Sci.*, **52**(2), pp. 334–338.
- [150] Song, J., and Curtin, W. A., 2012, “Atomic Mechanism and Prediction of Hydrogen Embrittlement in Iron,” *Nat. Mater.*, **12**(2), pp. 145–151.
- [151] Kuhr, B., Farkas, D., and Robertson, I. M., 2016, “Atomistic Studies of Hydrogen Effects on Grain Boundary Structure and Deformation Response in FCC Ni,” *Comput. Mater. Sci.*, **122**, pp. 92–101.

- [152] Adlakha, I., and Solanki, K. N., 2016, "Critical Assessment of Hydrogen Effects on the Slip Transmission across Grain Boundaries in α -Fe," Proc. R. Soc. A, **472**(2185), p. 20150617.
- [153] Lee, T. C., Robertson, I. M., and Birnbaum, H. K., 1990, "In Situ Transmission Electron Microscope Deformation Study of the Slip Transfer Mechanisms in Metals," Metall. Trans. A, **21**(9), pp. 2437–2447.
- [154] Cui, B., Kacher, J., Bertsch, K., Wang, S., McMurtrey, M., Was, G., Nagao, A., Martin, M., Sofronis, P., and Robertson, I. M., 2014, "Dislocation Interactions with Grain Boundaries," *35th Risø International Symposium on Materials Science, New Frontiers of Nanometals*, Roskilde, Denmark, September 1-5, 2014.
- [155] Chateau, J. P., Delafosse, D., and Magnin, T., 2002, "Numerical Simulations of Hydrogen-Dislocation Interactions in Fcc Stainless Steels. Part II: Hydrogen Effects on Crack Tip Plasticity at a Stress Corrosion Crack," Acta Mater., **50**(6), pp. 1523–1538.
- [156] Sofronis, P., Liang, Y., and Aravas, N., 2001, "Hydrogen Induced Shear Localization of the Plastic Flow in Metals and Alloys," Eur. J. Mech. A/Solids, **20**(6), pp. 857–872.
- [157] Liang, Y., Sofronis, P., and Aravas, N., 2003, "On the Effect of Hydrogen on Plastic Instabilities in Metals," Acta Mater., **51**(9), pp. 2717–2730.
- [158] Hirth, J. P., 1980, "Effects of Hydrogen on the Properties of Iron and Steel," Metall. Trans. A, **11**(6), pp. 861–890.
- [159] Liang, Y., Ahn, D. C., Sofronis, P., Dodds Jr., R. H., and Bammann, D., 2008, "Effect of Hydrogen Trapping on Void Growth and Coalescence in Metals and Alloys," Mech. Mater., **40**(3), pp. 115–132.
- [160] Ahn, D. C., Sofronis, P., and Dodds Jr., R. H., 2007, "On Hydrogen-Induced Plastic Flow Localization during Void Growth and Coalescence," Int. J. Hydrogen Energy, **32**(16), pp. 3734–3742.
- [161] Koplik, J., and Needleman, A., 1988, "Void Growth and Coalescence in Porous Plastic Solids," Int. J. Solids Struct., **24**(8), pp. 835–853.
- [162] Pardoen, T., and Hutchinson, J. W., 2000, "An Extended Model for Void Growth and Coalescence," J. Mech. Phys. Solids, **48**(12), pp. 2467–2512.
- [163] Ahn, D. C., Sofronis, P., and Dodds Jr., R. H., 2007, "Modeling of Hydrogen-Assisted Ductile Crack Propagation in Metals and Alloys," Int. J. Fract., **145**(2), pp. 135–157.
- [164] Novak, P., Yuan, R., Somerday, B. P., Sofronis, P., and Ritchie, R. O., 2010, "A Statistical, Physical-Based, Micro-Mechanical Model of Hydrogen-Induced Intergranular Fracture in Steel," J. Mech. Phys. Solids, **58**(2), pp. 206–226.
- [165] Smith, E., 1966, "The Nucleation and Growth of Cleavage Microcracks in Mild Steel," *Proceedings of Conference on Physical Basis of Yield and Fracture*, A.C. Stickland, ed., Institute of Physics and Physics Society, Oxford, pp. 36–46.
- [166] Nagao, A., Dadfarnia, M., Somerday, B. P., Sofronis, P., and Ritchie, R. O., 2018, "Hydrogen-Enhanced-Plasticity Mediated Decohesion for Hydrogen-Induced Intergranular and 'Quasi-Cleavage' Fracture of Lath Martensitic Steels," J. Mech. Phys. Solids, **112**, pp.

403–430.

- [167] Nagao, A., Martin, M. L., Dadfarnia, M., Sofronis, P., and Robertson, I. M., 2014, “The Effect of Nanosized (Ti,Mo)C Precipitates on Hydrogen Embrittlement of Tempered Lath Martensitic Steel,” *Acta Mater.*, **74**, pp. 244–254.

